The impacts and challenges of water use of electric power production in China

Jin, Y.

Chapter 7

Supplementary Information

7.1 Supplementary information to chapter 2

7.1.1 Methodologies

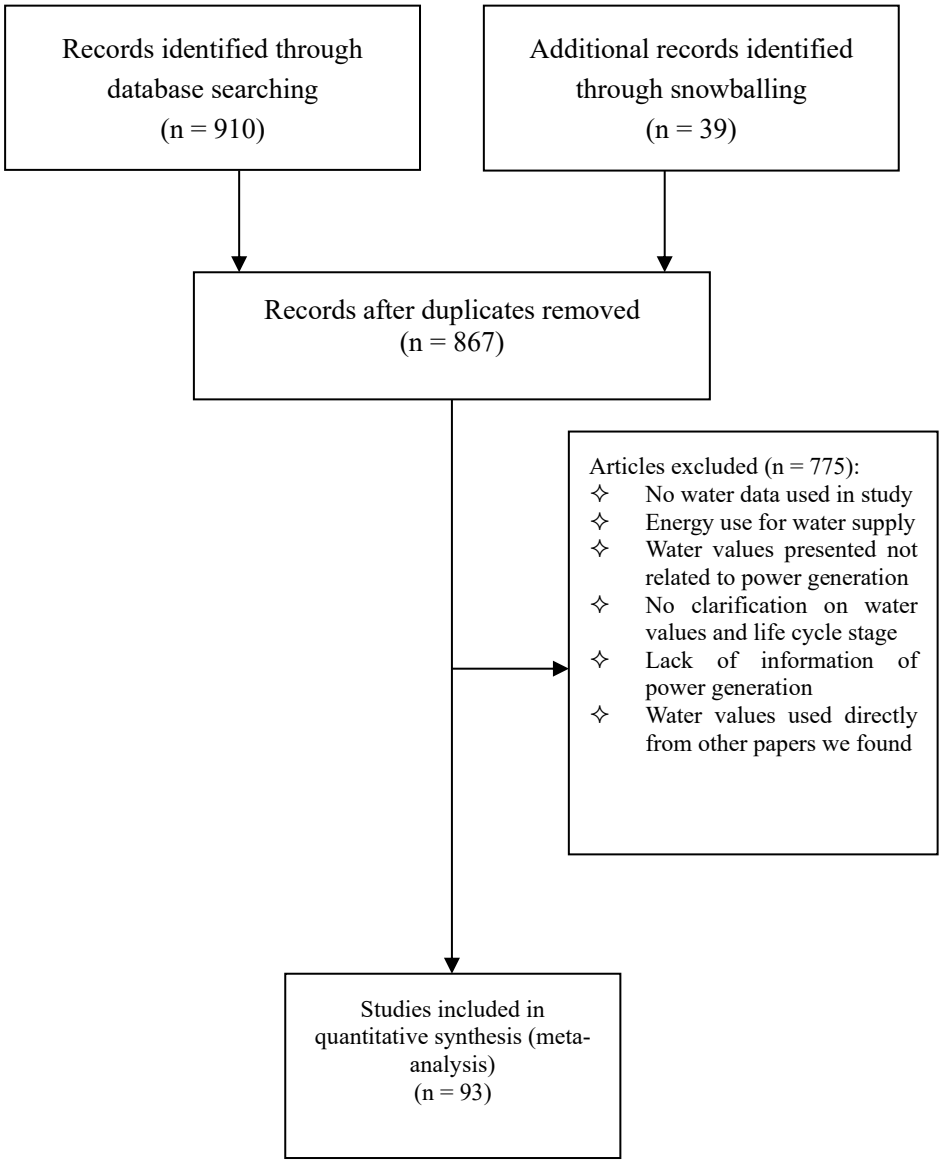

Figure S7.1.1 Flow diagram of meta-analysis.

Table S7.1.1 Search terms used in meta-analysis for each database

Database	Code
Web of Science	TS=(electricity) AND TS=("renewable*" OR "non*renewable*" OR "fossil fuel*" OR coal OR oil OR "natural gas" OR "shale gas" OR nuclear OR "hydro" OR "hydropower" OR biomass OR biofuel OR geothermal OR wind OR solar OR photovoltaic) AND TS=("water footprint" OR "water use" OR "water consumption" OR " water withdrawal" OR "water demand" OR "water requirement") AND LANGUAGE:(English)
ScienceDirect	(ttl(electricity AND (coal OR oil OR "natural gas" OR nuclear OR "hydro" OR "hydropower" OR biomass OR geothermal OR wind OR solar)) OR (key(electricity AND (coal OR oil OR "natural gas" OR nuclear OR "hydro" OR "hydropower" OR biomass OR geothermal OR wind OR solar)) AND (ttl("water footprint" OR "water use" OR "water consumption" OR "water withdrawal" OR "water requirement" OR "water demand")) AND Article types:(Research articles OR Book chapters OR Data articles)

The operational stage is the focus in previous studies, and the operational water consumption shows the great agreement when grouped by cooling types. In addition to the cooling type, unit type is another determinant of operational water consumption [139], and its main manifestation is the conversion efficiency [65]. Both the changes in cooling type and conversion efficiency would lead to the changes in operational water consumption. Particularly, the effects of changing conversion efficiency on water consumption differ across cooling types, e.g. the 1% change of conversion efficiency is expected to result in more water-saving amounts for closed-loop cooling than for dry cooling due to their different ways and scale of water consumption. Zhang et al. (2014) [139] investigated the relations between operational water consumption and its influencing variables (cooling type and unit type) for coal power plants. The effects of both cooling type and the conversion efficiency on the operational water consumption were considered in this study. In our study, five power types (coal, natural gas, oil, nuclear and biomass) were considered in the model without distinction since their operational water consumption have similar

characteristics and shows great agreement when grouped by cooling type as opposed to fuel type (Figure 2.2), the model is expressed as follows:

$$WC_i = \alpha_0 + \alpha_1 CT_{1,i} + \alpha_2 CT_{2,i} + \left(\sum_k \beta_k C_{i,k}\right) CE_i + \varepsilon_i \quad \text{(S7.1.1)}$$

In which,

$$CT_{1,i} = \begin{cases} 1, & once-through\ cooling \\ 0, & others \end{cases} \quad \text{(S7.1.2)}$$

And,

$$CT_{2,i} = \begin{cases} 1, & closed-loop\ cooling \\ 0, & others \end{cases} \quad \text{(S7.1.3)}$$

Through this model, the operational water consumption for once-through cooling, closed-loop cooling, and dry cooling can be expressed by eq (S4), eq (S5), and eq (S6), respectively:

$$WC_i = \alpha_0 + \alpha_1 + \beta_1 CE_i + \varepsilon_i \quad \text{(S7.1.4)}$$

$$WC_i = \alpha_0 + \alpha_2 + \beta_2 CE_i + \varepsilon_i \quad \text{(S7.1.5)}$$

$$WC_i = \alpha_0 + \beta_3 CE_i + \varepsilon_i \quad \text{(S7.1.6)}$$

Where WC_i represents the operational water consumption of sample i. the unit of WC_i (L/MWh). CE_i represents the conversion efficiency of sample i, with the unit: %. Three types of cooling are distinguished, i.e., once-through cooling, closed-loop cooling, and dry cooling. $CT_{1,i}$ is a binary variable that indicates the cooling type used by sample i: 1 for once-through cooling, 0 for other cooling types (closed-loop cooling and dry cooling). $CT_{2,i}$ is a binary variable that indicates the cooling type used by sample i: 1 for closed-loop cooling, 0 for other cooling types (once-through cooling and dry cooling). Dry cooling type is the baseline here.

Subscript k represents cooling types. $C_{i,k}$ is a binary variable that indicates the cooling type of sample i. If sample i belongs to cooling type k, then $C_{i,k}$ is designated as 1; otherwise $C_{i,k}$ is designated as 0.

α_0, α_1, α_2, and β_k are parameters to be estimated. α_0 is a constant parameter. β_k represents the contribution of the variance of conversion efficiency to the reduction of water consumption for power generation with cooling type k. ε_i represents the random error.

7.1.2 Water use of global power generation

Meldrum et al. (2013) reviewed the life cycle water consumption and water withdrawal of power production in the USA and harmonized the estimates from the literature [65]. Since most estimates in previous studies are not accompanied by enough information for harmonization, many studies could not be included in the review. All the estimates of coal thermal power were harmonized to the thermal efficiency of a sub-critical pulverized coal power plant; all the estimates of natural gas thermal power were harmonized to the thermal efficiency of a combined cycle plant. As a result, the water use estimates of coal power could be higher due to the low efficiency of sub-critical generating units compared to other coal power technologies (e.g. sup-critical); the water use estimates of natural gas power could be lower due to the high efficiency of combined cycle plant compared to other natural gas power technologies (e.g. steam cycle).

For biomass, the water use of fuel cycle was often expressed as water use from irrigation or precipitation instead of water consumption or water withdrawal. In this study, referring to the expression in [76, 85-88, 165, 341], the water use of biomass is presented as blue water consumption, with precipitation excluded as we study blue water only. [58, 165] estimated both blue and green water consumption for biomass power from the perspective of global average. Based on their results, the ratio of blue water to the total water consumption was obtained and can be used to adjust the water consumption of biomass power in [75, 85] to the blue water consumption. Both [75, 85] focused on the biomass in Canada and the USA. Mathioudakis et al. (2017) provided both blue water (15840 L/MWh) and green water (186480 L/MWh) of the fuel cycle of corn stover for power production through direct combustion [165]. The total value of blue and green water is comparable to the counterpart in [85], where the value is 256600 L/MWh. Besides, the heat content (17.55 MJ/kg and 18 MJ/kg, respectively) and moisture content (15%, 15%, respectively) of corn stover in both studies are very close. The ratio of blue water to the total water consumption for corn stover is used to adjust the water consumption of corn stover in [85] to the blue water consumption. The blue and green water consumed by pine in [75] were separated using the ratio in [165]. For wheat straw, there are two values of the proportion of blue water in [165], and both of them are 0.27. This proportion is used to separate the blue water from the sum of blue and green water in [75, 85].

Coefficient of variation of life cycle water consumption was calculated as shown in **Table S7.1.2**.

Table S7.1.2 Coefficient of variation (CV) of life cycle water consumption for each power type and technology

Power type	Cooling type	Generating technology	CV (%)
Coal	CL	IGCC	24
Coal	CL	SBC	19
Coal	CL	SPC	23
Coal	CL	USPC	23
Coal	DC	IGCC	14
Coal	DC	SBC	13
Coal	DC	SPC	13
Coal	DC	USPC	13
Coal	OT	SBC	29
Coal	OT	SPC	13
Natural Gas	CL	CC	44
Natural Gas	CL	ST	23
Natural Gas	DC	CC	72
Natural Gas	DC	ST	70
Natural Gas	OT	CC	24
Natural Gas	OT	ST	7
Oil			75
Nuclear	OT	ST	24
Biomass	CL	ST	68
Biomass	DC	ST	77
Biomass	OT	ST	76
Geothermal	DC	EGS-B	89
Geothermal	DC	HT-B	90
Geothermal	HD	HT-B	32
Geothermal	WC	HT-F	23
CSP	DC	Power tower	53
CSP	DC	Trough	46
CSP	HD	Power tower	58
CSP	HD	Trough	52
CSP	WC	Fresnel	10
CSP	WC	Power tower	30
CSP	WC	Trough	13
PV			68
Wind			119
Hydropower			634

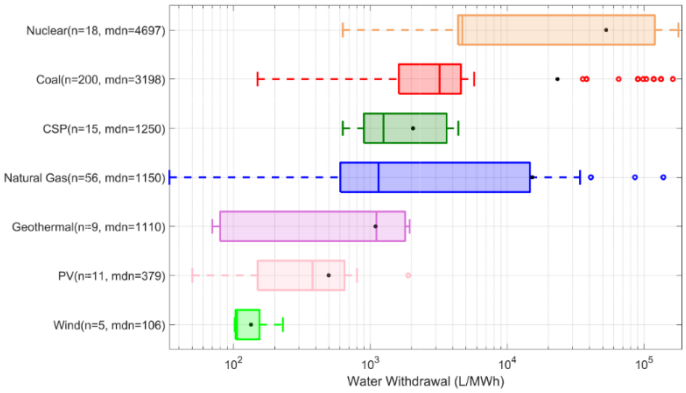

Figure S7.1.2 Life cycle blue water withdrawal for each type of power production. Water withdrawal is visualized on a log scale. The annotation mdn gives the median value of water consumption for each fuel type. The circles represent the outliers while the dots represent the mean for each power type. Hydropower, and biomass are excluded in this figure because the data of their life cycle water withdrawal were not available.

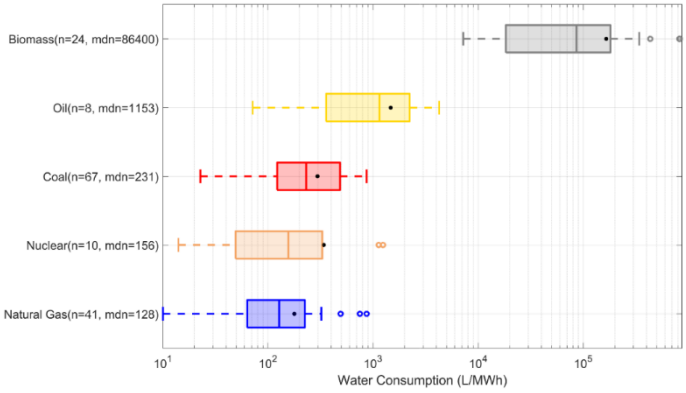

Figure S7.1.3 Blue water consumption in the fuel cycle. The value of water consumption for biomass power from [86] is particularly large (see below) and not included in the figure.

Dominguez-Faus et al. (2009) assessed the irrigation water requirements of corn ethanol and soybean biodiesel used for power generation. Corn ethanol consumed 2.27×10^6 to 8.67×10^6 liters of irrigation water for 1 MWh of power generation. Soybean biodiesel consumed 1.39×10^7 to 2.79×10^7 liters of irrigation water for 1 MWh of power generation [86].

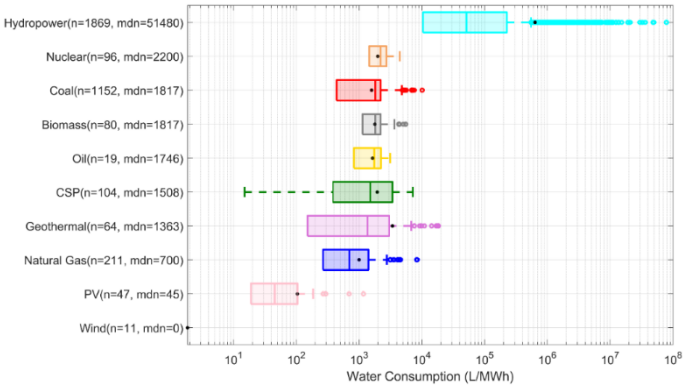

Figure S7.1.4 Blue water consumption of operation. For hydropower, the manifestation of the water use is water evapotranspiration, which is regarded as water consumption, as hydroelectric power generation does not withdraw or divert water [64]. For wind power, a boxplot is not used since most of the values are zero; the median and mean values are 0 and 1.85, respectively. For power types except CSP, their minimum water consumption of operation is zero and the values of q_1 - 1.5×(q_3-q_1) are negative. Thus, values between q_1 and zero are not recognized as outliers. The left whiskers of boxplots extend from q_1 to zero, with all the values between q_1 and zero contained. These left whiskers are not shown in this figure for simplicity.

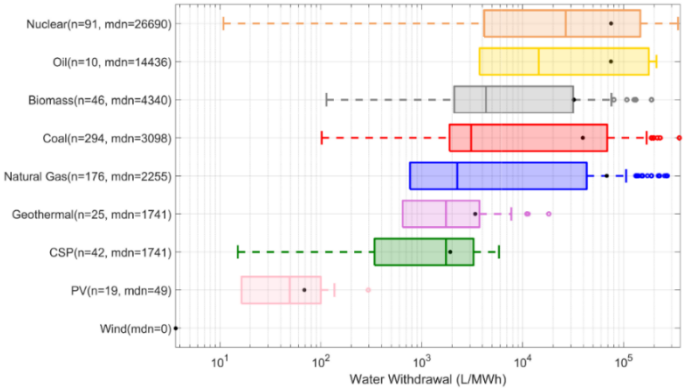

Figure S7.1.5 Blue water withdrawal of operation.

For consistency, the cooling type for coal, natural gas, oil, nuclear and biomass falls into closed-loop (CL), once-through (OT) and dry cooling (DC) referring to [22, 77, 89, 90, 92, 124, 131, 139, 342, 343]; Cooling type falls into wet cooling (WC), hybrid cooling (hybrid) and dry cooling (DC) for geothermal and CSP, referring to [104, 121, 344-351].

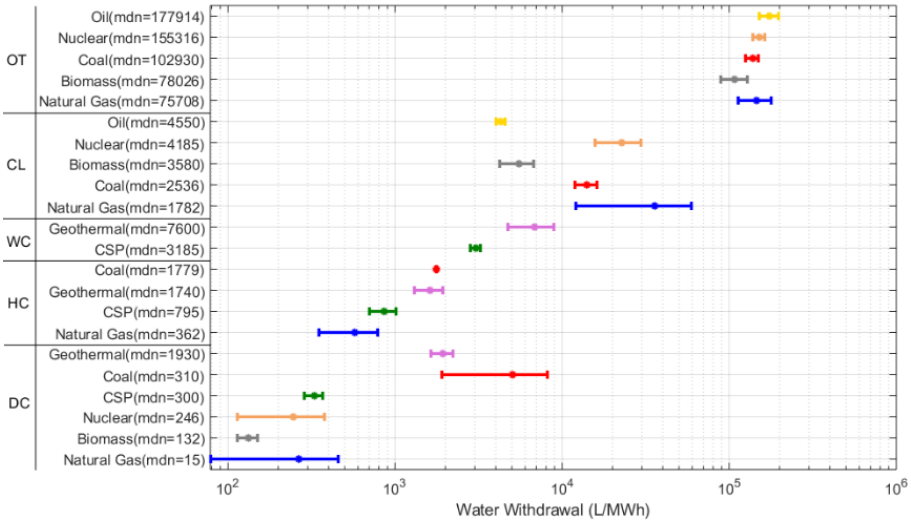

Figure S7.1.6 Blue water withdrawal of operation distinguished by power type and cooling type. The dots represent mean water consumption while the line segments represent the standard error of mean. The annotation mdn gives the median value. Hydropower, wind and PV do not have cooling needs and are not included. WC denotes wet cooling, CL denotes closed-loop cooling, HC denotes hybrid cooling (combining wet and dry cooling); OT denotes once-through cooling, and DC denotes dry cooling.

Water consumption (WC) and water withdrawal (WW) are usually calculated as a function of the lifetime of a power plant. However, the values of lifetime generally came from assumptions, as it is unavailable for plants under operation. The differences in the lifetime assumptions within the same power type makes the estimates less comparable. Therefore, we normalized the WC and WW to the same lifetime assumption if the estimates were provided with lifetime information for the power type. Otherwise, the original WC and WW were used. The normalization is conducted by assuming the water use changes proportionally to the lifetime [65]. Most frequently used lifetimes in the literature are used for normalization. Lifetimes used for normalization are shown in Table S7.1.3. WC estimates for power types including nuclear, wind and PV provided the same lifetime value, thus normalization is not needed within these power types. Only estimates for geothermal, natural gas and coal are normalized referring to the lifetime most frequently used in studies. The results are shown in Figure S7.1.7 and Figure S7.1.8.

Table S7.1.3 The lifetime value used in WC and WW estimates for each power type (unit: years)

Power type	Coal	Natural Gas	Nuclear	Geothermal	Wind	CSP	PV	Hydropower	Oil	Biomass
Lifetime for WC	30	30	40	30	20	30	30	NA	NA	NA
Lifetime for WW	30	30	40	30	NA	NA	NA	40	/	/

Note: NA indicates not all the estimates were provided with lifetime information for that power type, thus normalization was not conducted. No data of water withdrawal were available for oil. There is no water withdrawal for biomass since the water requirement of biomass is considered as water consumption in this study. [65] and [91] provided the lifetime of coal- and natural gas plant. The lifetimes of these two types of plant in this study referred to the values in [65] where the lifetimes were determined based on a review of published literature.

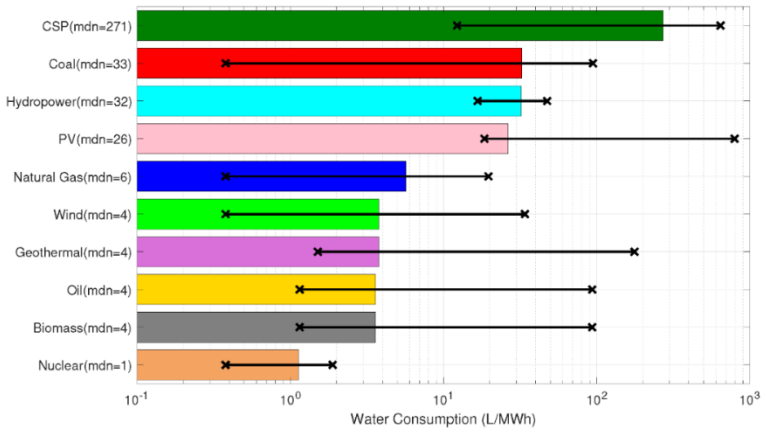

Figure S7.1.7 Blue water consumption of plant infrastructure. The bar shows the median water consumption, while the symbol 'x' represents the minimum and maximum water consumption in plant infrastructure for each power type. The minimum water consumption of wind power was derived from [65] where the value was described as 'less than 0.1 gal/MWh' instead of a precise value. It is assumed to be 0.1 gal/MWh (i.e. approximately 3.79 L/MWh) here. Some of the original values of water consumption were adjusted according to the lifetime of the power plant.

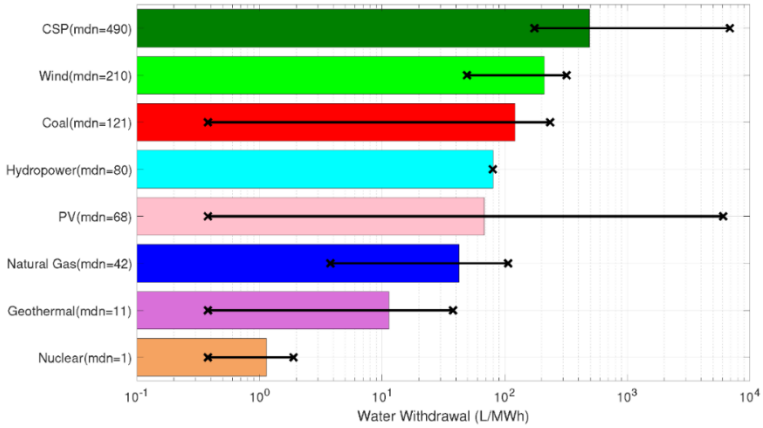

Figure S7.1.8 Blue water withdrawal of plant infrastructure. The bar shows the median water consumption, while the symbol 'x' represents the minimum and maximum water consumption in plant infrastructure for each power type. Only one value of water withdrawal for hydropower was available, which was derived from [64].

7.1.3 Water use of power generation at country level

The median operational water consumption for each country and power type are shown in Figure 7.1.5. For power plants with cooling needs, only wet cooling technologies (closed-loop, once-through and hybrid cooling technology) are included in Figure 7.1.5 since dry cooling is an obviously water-saving cooling technology for all countries, and wet cooling technologies account for 81% of the estimates extracted from the literature. The water consumption and water withdrawal for power generation at each life cycle stage are aggregated at country level. The median, minimum, and maximum values for countries mostly investigated in existing studies are shown in Tables S7.1.4-S7.1.8.

At the plant infrastructure stage, all the studies on the water consumption only focused on the USA, except [96] in which the water consumption for the hydropower station construction has been investigated. The water withdrawal for plant infrastructure of CSP in China is as high as 6863 L/MWh [158] where the material inputs within the whole economic system have been incorparated into the assessment by using a hydrid method. Similarly, the large water withdrawal for plant infrastructure of coal- and gas-supported power generation were obtained from [91] where an economic input-output life cycle assessment tool was employed.

Table S7.1.4 Country-specific blue water consumption of the fuel cycle (L/MWh)

Power Type	Country/Region	Median	Min	Max
Biomass	EU	10,800	7,200	14,400
Biomass	USA	435,600	435,600	435,600
Coal	Spain	120	26	130
Coal	USA	216	23	871
Coal	Canada	238	65	704
Coal	China	246	233	285
Natural Gas	Spain	28	10	45
Natural Gas (Con)	USA	83	23	220
Natural Gas (SG)	USA	222	64	871
Natural Gas (SG)	China	622	492	751
Nuclear	France	48	45	50
Nuclear	USA	212	14	1,249
Oil	Spain	891	281	1,500
Oil (Con)	USA	1,019	72	1,966
Oil (Oil Sand)	USA	1,658	806	2,509
Oil (Oil Shale)	USA	2,342	436	4,248

Note: median denotes median value; min denotes minimum value; max denotes maximum value. Con denotes conventional gas/oil, SG denotes shale gas. The data for Spain contain the water use of fuel production and processing, but not transportation, which is also a determinant of the water use of fuel cycle.

At the operational stage, the only study on the natural gas power in Egypt [352] did not clarify the turbine type of power plant, but the plant studied had similar characteristics of water consumption with combined cycle power plants according to the estimates for other countries. Egypt does not have operable nuclear power plants; Kotb and Abdelaal (2018) estimated the water consumption of nuclear power by scenario analysis [352]. China does not have operable inland nuclear power plants; Guo et al. (2012) and Chen et al. (2010) might made assessment based on research reactors [125, 353]. For biomass power with closed-loop cooling, studies on the USA focused on the water required for cooling [56, 63, 110, 354]. Few research investigated the water consumption of biomass power in China. The two available studies [100, 168] were based on the results in [355], where the water withdrawal instead of water consumption was assessed, and the water used for wastewater processing was included into operational water consumption. The estimates for Spain was provided based on the data of the USA from [63], and consequently had a bias towards the characteristics of

water consumption in the USA.

Plants in coastal area can use sea water for cooling, but they also need some freshwater to produce demineralized water, which can be used in the water-steam cycle to drive the electricity generation turbine. Mertens et al. (2015) provided the freshwater consumption of CCGT (combined cycle gas turbine) for cooling tower in Italy (14 L/MWh) and once-through cooling in France (6.6 L/MWh) [173].

Table S7.1.5 Country-specific blue water consumption of operation (L/MWh)

Power type	country	median	min	max
Biomass	USA	1,355	0	5,076
Biomass	Spain	2,152	1,734	2,414
Biomass	China	3,955	2,400	5,530
CSP	USA	1,414	15	7,192
CSP	China	3,415	750	4,000
Coal	India	399	242	4,035
Coal	Canada	1,020	90	3,650
Coal	Egypt	1,150	400	1,900
Coal	Spain	1,552	756	1,815
Coal	USA	1,628	0	10,107
Coal	China	1,889	20	7,070
Coal	UK	1,953	1,193	3,557
Geothermal	USA	1,363	0	18,400
Hydropower	Norway	109	57	161
Hydropower	New Zealand	1,692	324	70,884
Hydropower	Austria	1,962	0	3,924
Hydropower	Spain	9,500	3,000	109,000
Hydropower	USA	11,150	38	210,000
Hydropower	China	23,760	0	15,243,480
Hydropower	Vietnam	24,840	5,040	133,452
Hydropower	DR Laos	49,932	3,708	3,103,200
Hydropower	Turkey	85,860	4,680	118,440
Hydropower	Brazil	133,200	93,600	172,800
Hydropower	Ethiopia	147,240	0	750,240
Hydropower	Egypt	356,500	329,000	6,249,960
Hydropower	Thailand	552,312	1,548	3,160,872
Hydropower	India	1,273,000	1,273,000	1,273,000
Hydropower	Ghana	2,656,080	2,656,080	2,656,080
Natural Gas	Egypt	550	400	700
Natural Gas	Spain	684	0	1,814
Natural Gas	Belgium	722	13	1,431
Natural Gas	USA	795	0	8,438
Nuclear	China	130	40	3,682
Nuclear	Egypt	1,750	1,000	2,500
Nuclear	USA	2,197	0	4,452
Nuclear	Spain	2,590	1,020	3,460
Oil	USA	2,214	698	3,130

Oil	Spain	1,216	0	1,814
Oil	Egypt	800	800	800
PV	China	19	19	19
PV	USA	44	0	1,173
PV	Egypt	100	100	100
Wind	China	0	0	0
Wind	Egypt	0	0	0
Wind	USA	0	0	8

Table S7.1.6 Country-specific blue water withdrawal of operation (L/MWh)

Power type	country	median	min	max
Biomass	USA	3,324	114	189,384
Biomass	China	4,459	3,430	5,530
Biomass	Spain	31,647	1,734	189,600
CSP	USA	1,741	15	5,853
Coal	Canada	1,935	110	199,110
Coal	USA	4,486	102	457,895
Coal	India	5,255	500	159,000
Coal	China	7,610	320	521,251
Coal	Egypt	43,905	2,310	85,500
Geothermal	USA	2,158	0	18,110
Natural Gas	Italy	2,100	2,100	2,100
Natural Gas	Belgium	2,160	1,070	3,250
Natural Gas	USA	2,332	0	1,944,873
Natural Gas	France	2,800	2,800	2,800
Natural Gas	China	4,540	568	79,500
Natural Gas	Spain	13,675	0	189,000
Natural Gas	Egypt	22,050	1,000	43,100
Nuclear	USA	9,842	114	230,000
Nuclear	France	72,318	72,318	72,318
Nuclear	Spain	75,362	1,890	347,200
Nuclear	Egypt	86,050	4,200	167,900
Nuclear	China	178,000	87,000	227,000
Oil	Egypt	1,030	1,030	1,030
Oil	Spain	24,322	0	189,000
Oil	USA	68,520	3,748	211,983
PV	USA	45	0	295
PV	Egypt	100	100	100
Wind	Egypt	0	0	0
Wind	USA	4	0	11

Table S7.1.7 Country-specific blue water consumption of plant infrastructure (L/MWh)

Power type	country	median	min	max
Biomass	USA	4	1	94
CSP	USA	271	12	644
Coal	USA	4	0	95
Geothermal	USA	4	2	177
Hydropower	Norway	33	17	71
Natural Gas	USA	2	0	4
Nuclear	USA	1	0	2
Oil	USA	4	1	94
PV	USA	26	19	795
Wind	USA	4	0	34

Table S7.1.8 Country-specific blue water withdrawal of plant infrastructure (L/MWh)

Power type	country	median	min	max
CSP	USA	375	175	644
CSP	China	6,863	6,863	6,863
Coal	USA	4	0	45
Geothermal	USA	11	0	38
Hydropower	USA	80	80	80
Natural Gas	USA	4	4	4
Nuclear	USA	1	0	2
PV	USA	68	0	6,057
Wind	USA	98	49	314
Wind	Denmark	200	170	320
Wind	Spain	210	210	210
Wind	Italy	250	250	250

Tables S7.1.9-S7.1.11 show the water consumption of the fuel cycle, the water consumption of operation, and the water withdrawal of operation in China, respectively. Tables S7.1.12-S7.1.14 show the water consumption of the fuel cycle, the water consumption of operation, and the water withdrawal of operation in the USA.

In China, the water use of the fuel cycle for shale gas is significantly larger than for coal [89], whereas in the USA they are comparable due to the relatively lower water input for extraction [356]. Replacing coal by conventional gas for power generation can achieve a significant decrease in the water use of the fuel cycle in the USA. At the

operational stage, apart from dry cooling, the minimum cooling water consumption and withdrawal in China are 130 L/MWh for nuclear with once-through cooling type and 2180 L/MWh for coal with closed-loop cooling type, respectively. In the USA, the minimum cooling water consumption and withdrawal are both around 360 L/MWh for NGCC (natural gas combined cycle) with hybrid cooling type. Particularly, water consumption of geothermal energy with wet cooling differs greatly, depending on both plant type and resources type. In previous studies, the values of water consumption of coal power plants in China were assumed to be comparable to the median values of corresponding ones in the USA [77, 357, 358], while the values of water withdrawal can vary between the similar plants in China and the USA according to this study. Both in China and the USA, the water use of renewables could exceed that of non-renewables when hydropower, biomass and CSP with wet cooling type are deployed because of their high water use either in fuel cycle or in operation.

Gao et al. (2018) [100] presented the operational water consumption for nuclear power plants with closed-loop cooling technology based on the data from [125, 353]. However, [100] did not provide the calculation process, and the data in [125, 353] would not result in the value in [100]. Therefore, we recalculated the operational water consumption according to [125, 353]. Chen et al. (2010) [353] did not provide the annual operating time of the nuclear power plant and we assume it to be the same as that (i.e. 8147 hours) in [125].

Table S7.1.9 Blue water consumption of the fuel cycle of each power type in China (L/MWh)

Power type	Median	Min	Max
Coal	246	233	285
Shale Gas	622	492	751

Table S7.1.10 Blue water consumption of operation of each power type in China (L/MWh)

Power type	Cooling type	Technology	Median	Min	Max
Coal	CL	IGCC	1,210	1,210	1,210
Coal	CL	USPC	1,873	842	2,269
Coal	CL	SPC	2,029	150	6,900

Coal	CL	SBC	2,174	668	4,043
Coal	CL	SHV	3,270	3,170	3,370
Coal	CL	HV	4,800	4,800	4,800
Coal	DC	USPC	327	242	430
Coal	DC	SBC	336	152	790
Coal	DC	SPC	368	180	717
Coal	OT	USPC	228	190	380
Coal	OT	SPC	310	180	3,000
Coal	OT	SBC	367	170	1,450
Coal	OT	SHV	1,380	1,190	1,570
Natural Gas	CL	ST	2,760	2,120	4,160
Natural Gas	OT	CC	587	76	1,136
Nuclear	CL		3,380	3,077	3,682
Nuclear	OT		74	40	130
CSP	DC		750	750	750
CSP	WC		3,650	3,180	4,000
Biomass	CL		3,955	2,400	5,530
PV			19	19	19
Wind			0	0	0
Hydropower			23,760	0	15,243,480

Table S7.1.11 Blue water withdrawal of operation of each power type in China (L/MWh)

Power type	Cooling type	Technology	Median	Min	Max
Coal	CL	SPC	2,180	2,000	11,470
Coal	CL	SBC	2,625	1,500	3,750
Coal	CL	FB	11,659	11,659	11,659
Coal	CL	LMP	11,848	11,848	11,848
Coal	DC	USPC	1,022	1,022	1,022
Coal	OT	SPC	504,595	504,595	504,595
Coal	OT	FB	512,923	512,923	512,923
Coal	OT	LMP	521,251	521,251	521,251
Natural Gas	CL	ST	4,540	4,540	4,540
Natural Gas	OT	CC	15,045	568	79,500
Nuclear	OT	ST	178,000	87,000	227,000
Biomass	CL		4,459	3,430	5,530

Table S7.1.12 Blue water consumption of the fuel cycle of each power type in the USA (L/MWh)

Power type	Median	Min	Max
Coal	216	23	871
Conventional Gas	83	23	220
Shale Gas	222	64	871
Conventional Oil	1,019	72	1,966
Oil Sand	1,658	806	2,509
Oil Shale	2,342	436	4,248
Nuclear	212	14	1,249
Biomass	435,600	435,600	435,600

Table S7.1.13 Blue water consumption of operation of each power type in the USA (L/MWh)

Power type	Cooling type	Technology	Median	Min	Max
Coal	CL	IGCC	1,620	132	3,140
Coal	CL	SPC	1,878	15	4,350
Coal	CL	FB	2,120	2,120	2,120
Coal	CL	SBC	2,875	757	5,030
Coal	DC	IGCC	227	189	265
Coal	OT	SPC	390	242	469
Coal	OT	SBC	475	269	1,325
Coal	OT	IGCC	625	510	740
Coal	OT	FB	872	795	950
Natural Gas	CL	CC	908	4	1,900
Natural Gas	CL	ST	2,506	19	8,438
Natural Gas	DC	CC	15	0	940
Natural Gas	DC	ST	57	0	114
Natural Gas	Hybrid	CC	360	326	757
Natural Gas	OT	CC	380	8	8,267
Natural Gas	OT	ST	1,200	246	2,358
Oil	CL		2,625	1,100	3,130
Oil	OT		1,100	910	2,233
Nuclear	CL		2,540	1,408	3,403
Nuclear	DC		151	0	265
Nuclear	OT		1,437	106	4,452
Biomass	CL	CC	1,515	1,120	2,080
Biomass	CL	ST	1,817	1,136	3,653
Biomass	DC	ST	0	0	114
Biomass	OT	CC	625	510	740
Biomass	OT	ST	1,136	1,136	1,249
CSP		Dish stirling	19	15	23
CSP	DC	Trough	297	121	625
CSP	DC	Power tower	415	98	606
CSP	Hybrid	Power tower	795	341	4,111
CSP	Hybrid	Trough	1,287	416	4,198
CSP	WC	Power tower	2,909	1,514	3,452
CSP	WC	Trough	3,683	2,120	7,192
CSP	WC	Fresnel	3,785	3,785	3,785
Geothermal	DC	EGS-O	0	0	0
Geothermal	DC	GP-B	76	0	151
Geothermal	DC	HT-B	303	151	1,022
Geothermal	DC	EGS-B	1,363	151	2,725
Geothermal	Hybrid	HT-F	1,200	1,200	1,200
Geothermal	Hybrid	HT-B	5,350	4,200	6,500
Geothermal	WC	EGS-F	0	0	0
Geothermal	WC	HT-F	95	0	14,300
Geothermal	WC	HT-O	8,350	6,800	9,900
Geothermal	WC	EGS-O	9,300	7,600	11,000
Geothermal	WC	HT-B	14,300	5,700	17,200
PV			44	0	1,173
Wind			0	0	8

Note: For geothermal, only freshwater consumed is included.

Table S7.1.14 Blue water withdrawal of operation of each power type in the USA (L/MWh)

Power type	Cooling type	Technology	Median	Min	Max
Coal	CL	IGCC	1,817	606	26,980
Coal	CL	FB	3,785	3,785	3,785
Coal	CL	SPC	4,156	2,196	57,200
Coal	CL	SBC	4,633	1,136	98,421
Coal	DC	IGCC	379	379	379
Coal	OT	IGCC	66,815	53,400	80,230
Coal	OT	FB	75,708	75,708	75,708
Coal	OT	SPC	85,552	85,365	87,064
Coal	OT	SBC	102,587	56,781	215,768
Natural Gas	CL	CC	1,098	53	172,520
Natural Gas	CL	ST	4,069	10	1,944,873
Natural Gas	DC	CC	15	0	379
Natural Gas	DC	ST	114	114	114
Natural Gas	Hybrid	CC	362	329	1,230
Natural Gas	OT	CC	75,708	27,255	266,190
Natural Gas	OT	ST	189,384	37,854	1,595,509
Oil	CL		4,550	3,748	4,550
Oil	OT		177,914	132,490	211,983
Nuclear	CL		4,168	1,893	171,960
Nuclear	DC		246	114	379
Nuclear	OT		145,595	80,304	230,000
Biomass	CL	ST	2,082	1,136	5,527
Biomass	CL	CC	10,090	1,480	26,980
Biomass	DC	ST	132	114	150
Biomass	OT	CC	66,815	53,400	80,230
Biomass	OT	ST	132,489	75,708	189,384
CSP	DC	Trough	282	125	625
CSP	DC	Power tower	454	98	606
CSP	Hybrid	Power tower	644	341	946
CSP	Hybrid	Trough	1,287	1,287	1,287
CSP	WC	Power tower	2,423	1,514	3,100
CSP	WC	Trough	3,577	2,196	4,997
Geothermal	WC	EGS-F	0	0	0
Geothermal	WC	EGS-O	9,300	7,600	11,000
Geothermal	WC	HT-O	9,500	7,700	11,300
PV			45	0	295
Wind			4	0	11

Note: For geothermal, only freshwater consumed is included.

7.1.4 Influencing factors of water use

From the literature, influencing factors of water consumption were collected for each lifecycle stage of power generation: for operational stage, conversion efficiency and capacity factor were investigated; for fuel cycle and plant infrastructure stage, heat

content of fuel and lifetime of plants was investigated, respectively. Tables S7.1.15-S7.1.18 show the values of these influencing factors in the literature.

Table S7.1.15 Conversion efficiency of each power type and technology

Power type	Technology	Median	Min	Max
Biomass	ST	25	16	38
Biomass	CC	37	37	59
Coal	FB	35	35	36
Coal	SBC	38	33	54
Coal	SPC	40	26	44
Coal	USPC	43	39	45
Coal	IGCC	45	39	45
CSP	Fresnel	10	9	11
CSP	Trough	15	9	16
CSP	Dish stirling	16	9	22
CSP	Power tower	20	9	20
Geothermal	EGS-B	9	9	9
Geothermal	HT-B	9	8	10
Geothermal	HT-F	11	11	11
Geothermal	DS	12	8	15
Natural gas	CT	33	30	33
Natural gas	ST	33	32	33
Natural gas	SC	40	40	40
Natural gas	CC	51	39	75
PV	Thin film	13	12	13
PV	c-Si	13	13	13
PV	Thin film, III-V	37	37	37
Nuclear		33	31	40
Oil		36	36	36
Wind		39	39	39

Table S7.1.16 Capacity factor of each power type

Power type	Median	Min	Max
CSP	48	22	56
Coal	85	75	90
Geothermal	95	95	95
Natural gas	85	80	85
Nuclear	92	92	92
PV	23	23	23
Wind	27.4	19	46

Table S7.1.17 Lifetime of each type of power plant

Power type	Median	Min	Max
Biomass	30	30	30
CSP	30	20	30
Coal	30	30	60
Geothermal	30	20	30
Natural gas	45	30	60
Nuclear	33	20	50
PV	30	30	30
Wind	20	20	20

Table S7.1.18 Heat content of fuel

Power type	Median	Min	Max
Biomass	17.83	13.45	20.00
Coal	20.64	16.28	27.14
Natural gas	53.54	49.61	55.00

The relations between influencing factors and water consumption were investigated by calculating their correlation coefficients, as shown in Table S7.1.19. For operational water consumption, conversion efficiency and capacity factor were investigated in this study; for water consumption of fuel cycle and plant infrastructure stage, heat content of fuel and life time of plants was investigated, respectively.

The negative signs of these coefficients show that in general, water consumption can be to some extent reduced by increasing the values of these factors. However, the coefficients cannot accurately measure the effects of these factors on water consumption, because variables influencing water consumption differed across different literature and could influence the coefficients. For example, fuel-cycle water consumption of conventional natural gas was larger in [92] than in [91]. This large difference in water consumption could be caused by different extraction approaches, burning conditions and other variables. Even within [92], The natural gas with the same heat content has different fuel-cycle water consumption. There are only two studies available for calculating correlation coefficients for both PV and CSP. Although the correlation coefficient shows the strong relations between water consumption and conversion efficiency, this relation is not reliable due to the unknown backgrounds of studies since the operational water consumption can be largely affected by other

various conditions, such as practical habit of panel cleaning, sunshine duration etc. Generally, water consumption can be to some extent reduced by increasing the values of these factors. However, the correlation coefficients cannot accurately measure the effects of these factors on water consumption due to other differences in previous studies that cannot be controlled in the analysis.

Meldrum et al. (2013) harmonized the results from the literature using assumed values for influencing factors and assuming water consumption changed proportionally to the values of factors. We could not obtain the original values of factors and water consumption, thus the results in [65] were not used in this section.

Table S7.1.19 Correlations between influencing factors and water consumption

Heat Content	Cooling Types	Correlation Coefficients
Coal	/	-0.14
Natural gas	/	-0.88
Conversion Efficiency		
Coal	CL	-0.12
Coal	DC	-0.29
Coal	OT	-0.03
CSP	DC	-0.20
Nuclear	CL	-0.68
Natural gas	OT	-0.27
Natural gas	DC	-0.71
Biomass	CL	-0.91
Natural gas	CL	-0.19
PV	/	-1.00
CSP	WC	1.00
Capacity Factor		
Coal	CL	-0.34
Life Time		
Geothermal	/	-0.58

Note: For natural gas power plants, only combined cycle units were investigated due to data limitation. For capacity factor, only coal power plants with sup-critical units were investigated.

The regression model (eq. A1-A6) was solved by “regstats” function in Matlab version 2018a. The residuals of regression model are distributed at the both sides of the line: residual = 0, as shown in Figure S7.1.9. The outliers are not discussed here since they are included in the analyses of other sections of this study. Besides, there is no reason to excluded outliers in previous studies for a better fitness of regression.

Table S7.1.20 Parameter estimation of the operational water consumption for power generation

Parameter	Estimation	p-value of t stats
α_0	742	0.00***
α_1	626	0.10*
α_2	2867	0.00***
β_1	-16.22	0.02**
β_2	-36.83	0.00***
β_3	-10.33	0.10*
Number of samples: 720		
R^2: 0.7442, adjusted R^2: 0.7424		
F: 415.37, and its p-value: 0.00		

Note: Significance symbol: *** p<=0.01, ** p<=0.05, *p<=0.1; k = 1 for once-through cooling, k = 2 for closed-loop cooling, and k = 3 for dry cooling.

Figure S7.1.9. The residual distribution of regression model.

For hydropower, the literature generally provided both key influencing factors of water use, i.e. reservoir area and evaporation rate. An analysis of variance was conducted to look at the effects of both factors on the operational water consumption of hydropower. Results (Table S7.1.21) showed that evaporation rate generally plays a more important role in determining the operational water consumption of

hydropower compared to reservoir area.

Table S7.1.21 Analysis of variance in hydropower

Source	Sum of Squares	F	Sig.
Reservoir area	6.46×10^{12}	133.84	0.00
Evaporation rate	1.19×10^{14}	2791.39	0.00
Error	6.99×10^{9}		
Total	3.70×10^{14}		

7.1.5 Uncertainties in methodological choice

Studies using Hybrid LCA focused on life cycle water consumption for power generation. The average values of life cycle water consumption estimates for PLCA and hybrid LCA method are shown in Table S7.1.22, respectively. Only PLCA was used for estimating water consumption for geothermal.

The water use of biomass and hydropower mainly originates from the direct water use, which is included in the LCI phase of both methods, indicating that the water use of these two power types is determined by the actual water use rather than assessment methods. The low estimates based on hybrid LCA for biomass and hydropower were assessed in [83], where both power types used low direct water consumption. Thus, the counterintuitive result occurs that estimates based on hybrid LCA is significantly lower than the counterparts based on conventional PLCA.

Table S7.1.22 The average values of life cycle blue water consumption estimates using PLCA and hybrid LCA methods

	Coal	Natural gas	Oil	Nuclear	Wind	CSP	PV
LCA	2,190	861	3,185	2,062	14	2,152	234
Hybrid LCA	2,537	1,229	3,220	3,100	633	2,400	1,295

For hydropower, approximately 25% of the world's reservoirs with a dam higher than 15 m serve multiple purposes [141], such as flood control, drinking water supply, irrigation, power production, recreation, navigation and more [94, 140]. The hydroelectric water use of a multi-purpose power station may be overestimated if a reservoir's water use is attributed entirely to power production [95]. Existing allocation models have been built based on the following allocation factors: the ranking of hydropower production among multiple purposes [24], the ratio of economic value of hydropower to the total economic value derived from the reservoir [141], the ratio of

water volume for hydropower to the total water volume for all the functions of a reservoir [359], and the ratio of power production of hydropower to the total power (power production of hydropower and lost power production due to other functions of a reservoir) [359].

Table S7.1.23 The range of allocation factors of water use for hydropower

	Economic allocation	Energy allocation	Volume allocation	Ranking of purpose
Min	0	0.02	0.02	0.33
Max	0.96	0.43	0.39	1.00

7.1.6 Uncertainties in system boundary delineation

Table S7.1.24 The ratio of blue water consumption per stage to life cycle water consumption (%)

	Fuel cycle	Plant infrastructure
Coal	3-38	~0-15
Nuclear	3-47	~0
Oil	9-64	~0-12
Natural gas	2-79	~0-1
Biomass	~100	~0
Hydropower	/	~0-46
CSP	/	8-91
PV	/	12-93
Wind	/	~0-~100
Geothermal	/	~0-~100

Note: Water withdrawal is not investigated because it is generally assumed to be equal to water consumption for fuel cycle and plant infrastructure. "~0" and "~100" means the ratio is approximate to 0 and 100, respectively. "a-b" means the ratio ranges from a to b.

Within the fuel cycle, there are two main sub-stages: fuel production and fuel transport. The former typically includes fuel extraction, processing, and often revegetation, while the latter are performed mainly in two ways for coal, gas, and oil: conventional transport (e.g. truck, train, shipping) and pipelines [65, 89-92, 169]. Compared to fossil fuels such as coal and natural gas, biomass has generally a lower energy density. Large amounts of biomass feedstock need to be transported from the field to the power plant. To reduce transport costs, biomass power plants are generally close to the field of biomass feedstock and highway transport is the primary transport mode

[360-362]. In this case, the water consumption is relatively small at this stage [360].

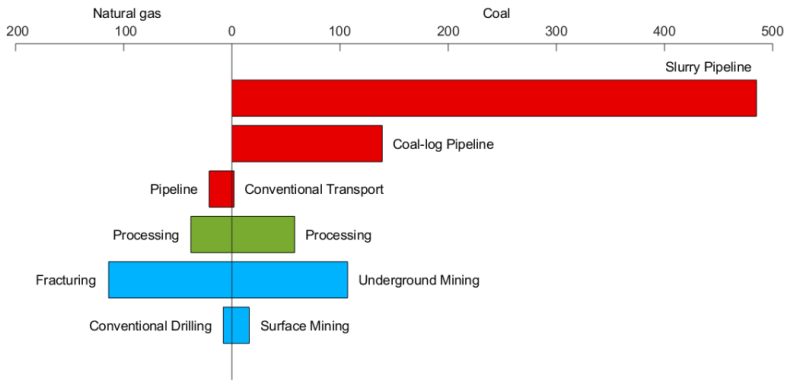

Figure S7.1.10 The median blue water consumption of the sub-stages of fuel cycle for coal and natural gas. Unit: L/MWh. For the range of water consumption, see Table S8.1.25 and Table S7.1.26.

Table S7.1.25 and Table S7.1.26 shows the water consumption (median, minimum, and maximum values) of sub-stages of fuel cycle for coal and natural gas, respectively. Detailed information within fuel cycle are not available for oil. The extraction approaches are generally used according to the existing state of resources. For coal, extraction approach can be further divided into: surface mining and underground mining [64, 90, 363, 364]. For natural gas, the extraction approaches are: conventional drilling and fracturing [65, 91, 92, 109]. For coal, the transport approach can be further categorized as: conventional transport (train, truck, shipping), coal-log pipeline, and slurry pipeline [90]. Coal slurry pipelines transport a slurry of water and pulverized coal over long distances and the ratio of coal to water is about 1 to 1 by weight [124, 365]. Coal-log pipelines works in the similar way as slurry pipelines, but the mass ratio of coal to water is lower-- is about 3:1 [90].

Table S7.1.25 Blue water consumption of coal fuel cycle (L/MWh)

Sub-stages of fuel cycle		Water consumption		
		Median	Min	Max
Extraction	Surface mining	16	2	49
	Underground mining	107	30	681
Processing		58	30	2785
Transport	Conventional transport	2	0.38	4
	Coal-log pipeline	139	117	150
	Slurry pipeline	485	379	1552

Table S7.1.26 Blue water consumption of natural gas fuel cycle (L/MWh)

Sub-stages of fuel cycle		Water consumption		
		Median	Min	Max
Extraction	Conventional drilling	8	0.38	72
	Fracturing (shale gas)	114	72	163
Processing		38	2	55
Transport	Pipeline	21	4	32

7.2 Supplementary information to chapter 3

Table S7.2.1 The capacity factor and its variation for electricity-generating units by region in 2017.

Provinces	Capacity factor	Standard deviation	Coefficient of variation
Anhui	0.71	0.05	6.40
Chongqing	0.69	0.10	15.29
Fujian	0.74	0.05	6.27
Gansu	0.68	0.06	9.05
Guangdong	0.70	0.06	8.06
Guangxi	0.66	0.11	17.20
Guizhou	0.72	0.05	7.45
Hainan	0.68	0.01	1.26
Hebei	0.71	0.12	16.23
Heilongjiang	0.62	0.06	10.31
Henan	0.64	0.07	11.09
Hubei	0.76	0.04	5.10
Hunan	0.63	0.06	10.15
Inner Mongolia	0.72	0.06	8.71
Jiangsu	0.72	0.04	5.22
Jiangxi	0.72	0.03	3.56
Jilin	0.58	0.03	5.25
Liaoning	0.61	0.07	11.04
Ningxia	0.70	0.07	9.39
Qinghai	0.75	0.06	8.02
Shaanxi	0.73	0.08	10.91
Shandong	0.74	0.05	6.23
Shanghai	0.66	0.08	11.90
Shanxi	0.70	0.04	6.22
Tianjin	0.69	0.05	6.71
Xinjiang	0.63	0.05	7.69
Yunnan	0.69	0.12	18.03
Zhejiang	0.72	0.04	5.12

Table S7.2.2 The descriptive statistics of electricity-generating units by region in 2017 in our database.

Provinces	Number of units	Installed capacity (MW)	Electricity output (GWh)	percentage of coal power (%)	percentage of hydropower (%)
Anhui	168	54963	248119	78	19
Beijing	22	2187	5222	22	72
Fujian	187	59689	273271	39	45
Gansu	143	28714	99048	65	35
Guangdong	307	102412	502646	63	25
Guangxi	191	50968	192730	34	57
Guizhou	195	50570	167709	52	47
Hainan	30	6082	26112	50	42
Hebei	202	52445	279989	93	7
Henan	261	75833	279662	85	13
Heilongjiang	102	20855	76039	95	0
Hubei	225	66208	240477	40	56
Hunan	176	32053	95201	33	62
Jilin	126	25162	62372	64	23
Jiangsu	318	94615	477357	86	2
Jiangxi	106	30951	139894	56	40
Liaoning	175	45012	202602	83	9
Inner Mongolia	386	109235	486316	100	0
Ningxia	95	32780	133836	90	10
Qinghai	54	13769	38609	23	77
Shandong	417	107724	435635	95	1
Shanxi	261	76283	304116	94	6
Shaanxi	182	54442	275537	82	18
Shanghai	35	15119	54777	89	0
Sichuan	192	36777	123620	17	83
Tianjin	38	14084	60525	100	0
Tibet	18	188	310	0	27
Xinjiang	293	66588	294537	93	7
Yunnan	216	49435	152169	19	79
Zhejiang	200	67577	317632	52	28
Chongqing	87	18829	58800	63	34

Table S7.2.3 Virtual water transfer and co-benefits on water-saving of power transmission unit: million m^3

Water sources		Water consumption	Water withdrawal
Surface water	Transfer	2086	6047
	Savings	1867	15806
	Co-benefits	-	+
Groundwater	Transfer	29	130
	Savings	37	490
	Co-benefits	+	+
Reclaimed water	Transfer	42	64
	Savings	103	178
	Co-benefits	+	+
Seawater	Transfer	15	5036
	Savings	91	28223
	Co-benefits	+	+

Note: '+' indicates power transmission decreases water use, '-' indicates power transmission increases water use.

Table S7.2.4 Short names of provinces.

Provinces	Short names	Provinces	Short names
Anhui	AH	Liaoning	LN
Beijing	BJ	Inner Mongolia	IM
Fujian	FJ	Ningxia	NX
Gansu	GS	Qinghai	QH
Guangdong	GD	Shandong	SD
Guangxi	GX	Shanxi	SX
Guizhou	GZ	Shaanxi	SHX
Hainan	HAIN	Shanghai	SH
Hebei	HEB	Sichuan	SC
Henan	HEN	Tianjin	TJ
Heilongjiang	HLJ	Xizang	TI
Hubei	HB	Xinjiang	XJ
Hunan	HN	Yunnan	YN
Jilin	JL	Zhejiang	ZJ
Jiangsu	JS	Chongqing	CQ
Jiangxi	JX		

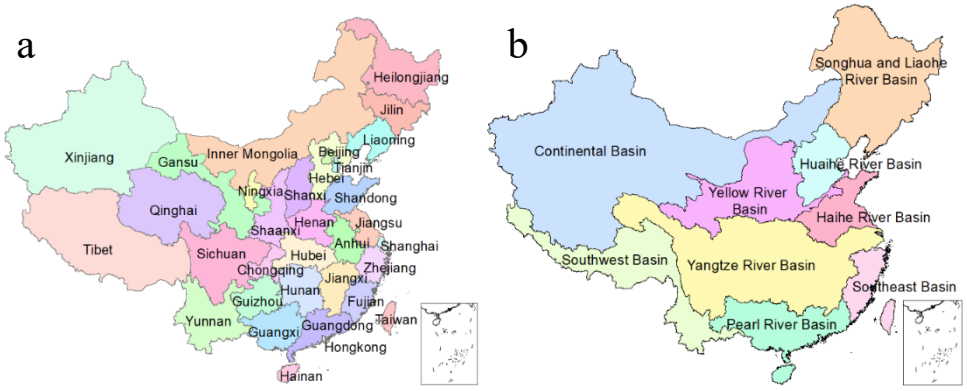

Figures S7.2.1 Map (a) presents provinces and map (b) shows the major river basins.

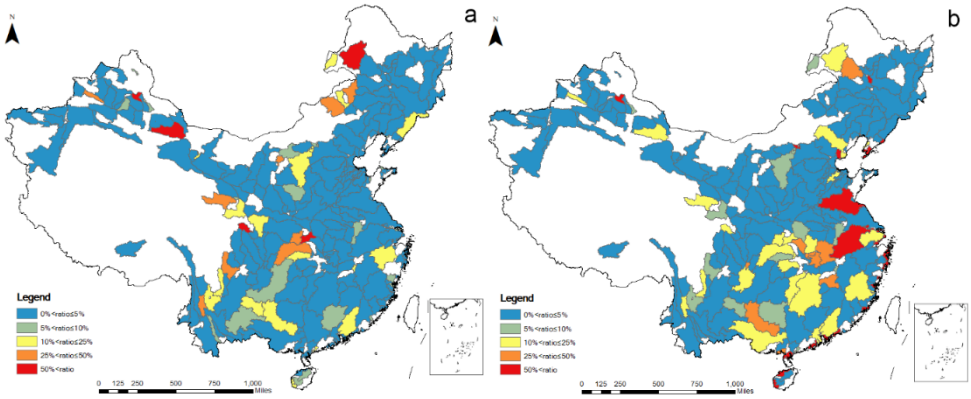

Figures S7.2.2 The ratio of water consumption of power production to the total water consumption (a) and the ratio of water withdrawal of power production to the total water withdrawal (b) at basin level in China in 2017.

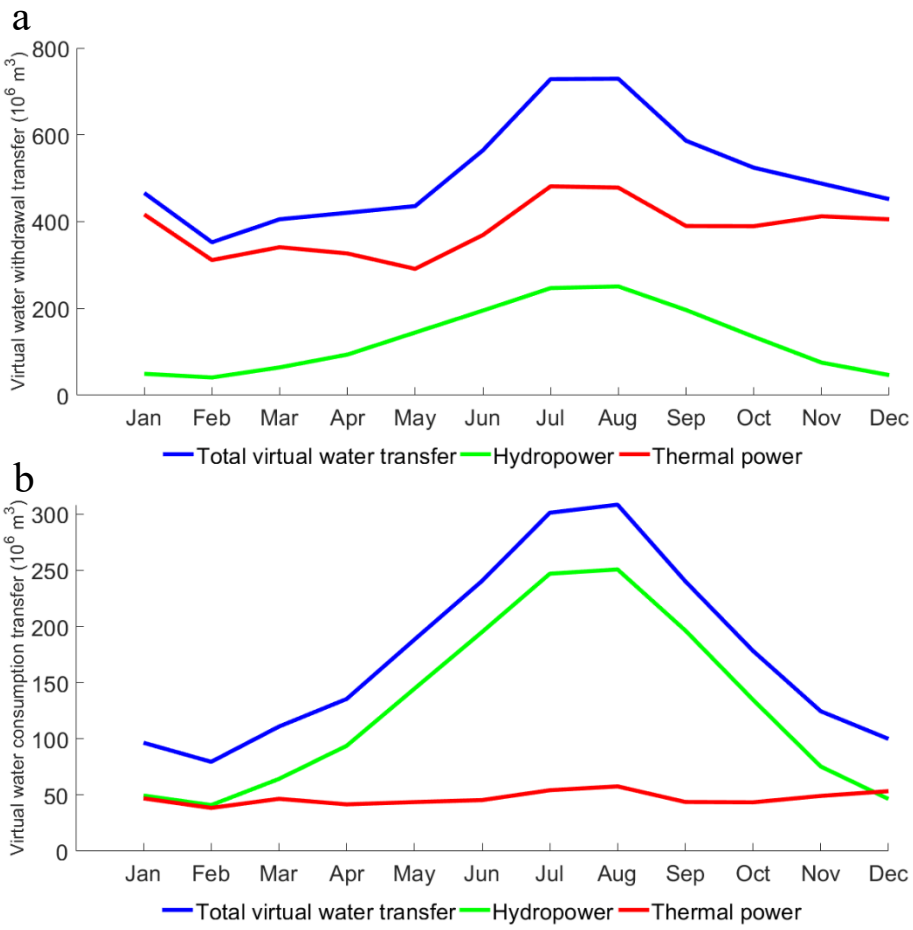

Figures S7.2.3 The monthly virtual water consumption (a) and withdrawal (b) transfers via hydropower and thermal power transmission in China.

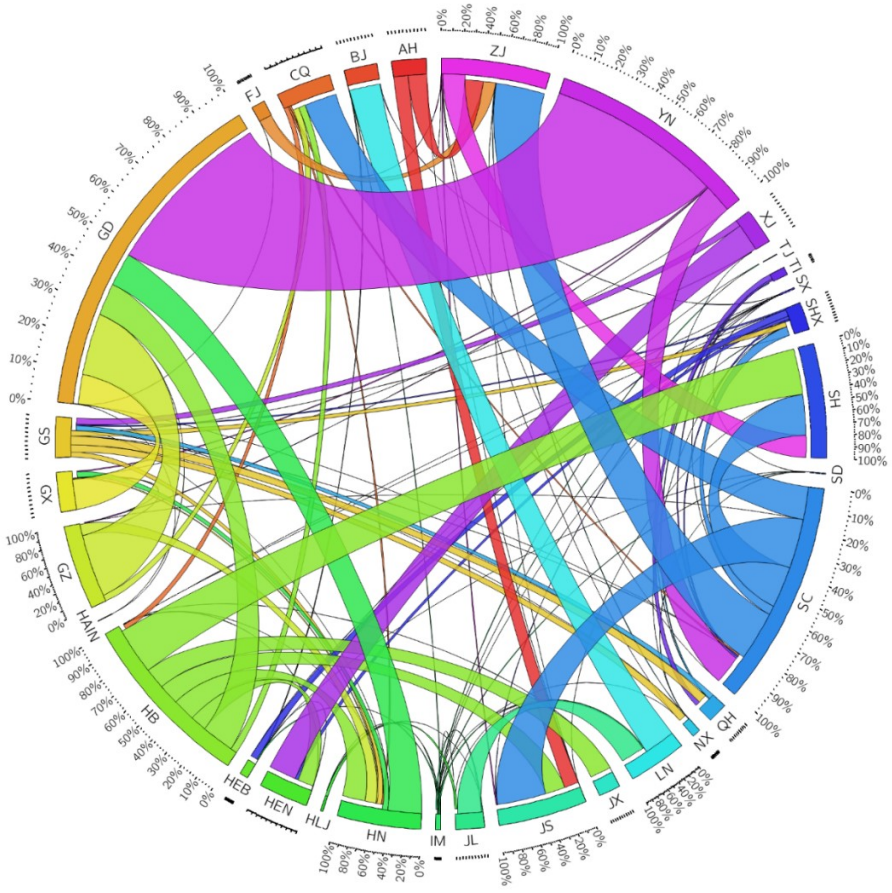

Figures S7.2.4 Virtual water consumption/withdrawal transfer via hydropower transmission. The full and short names of provinces are shown in **Figure S7.2.4.**

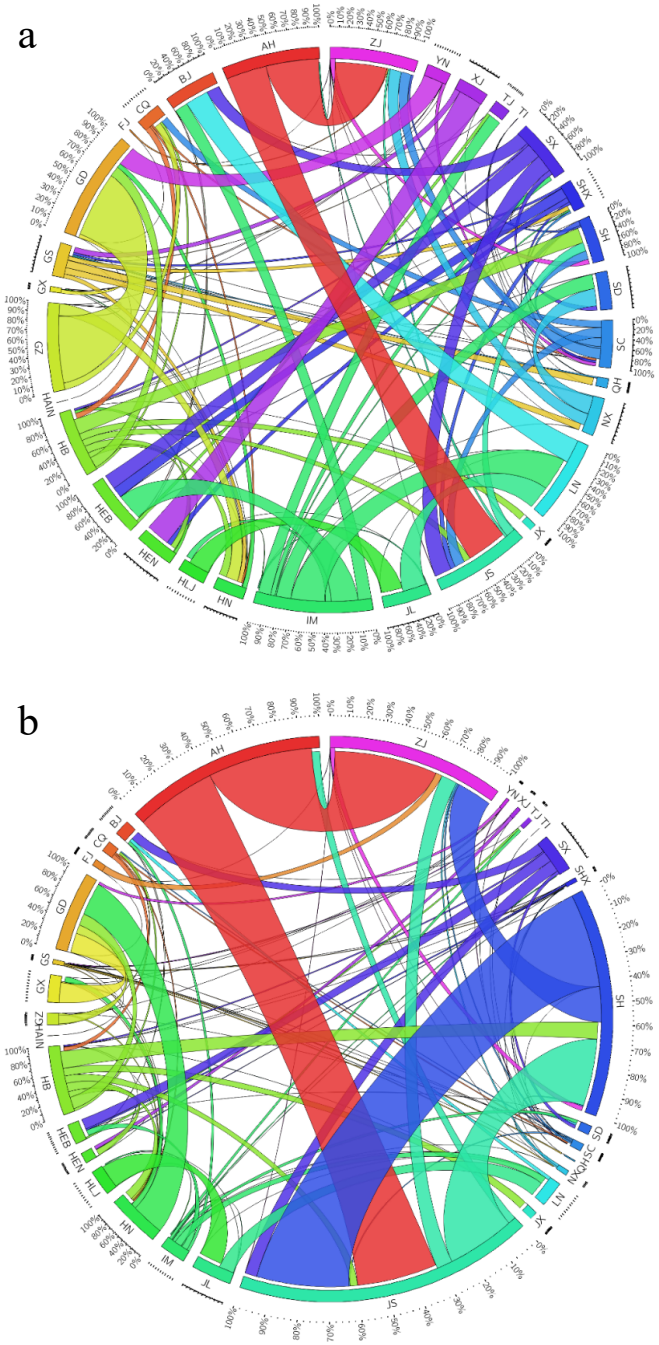

Figures S7.2.5 Virtual water consumption (a) and withdrawal (b) transfer via thermal power transmission.

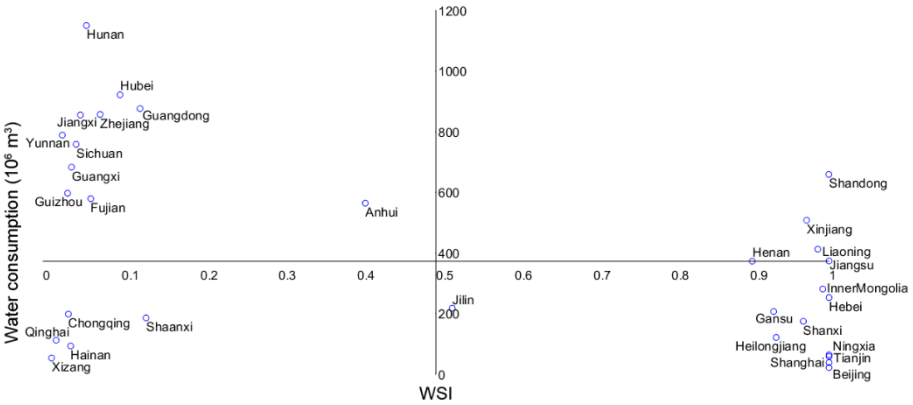

Figures S7.2.6 The provincial WSI and freshwater consumption.

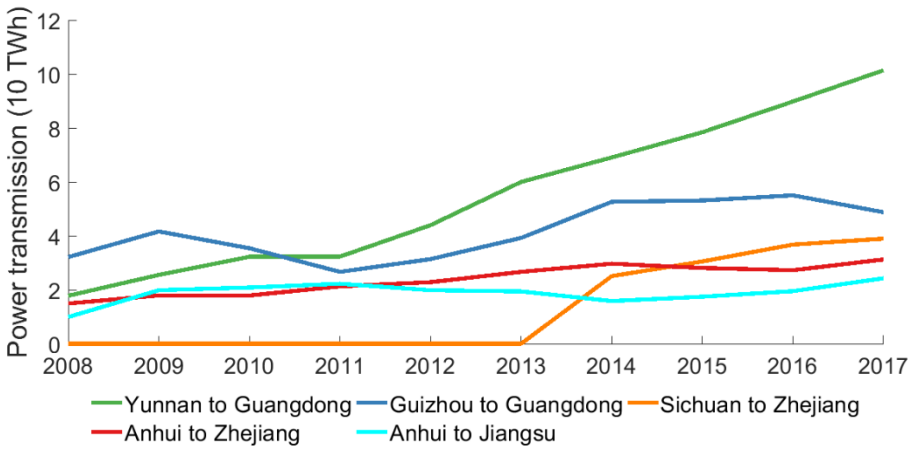

Figures S7.2.7 Power transmission of main corridors between provinces.

Construction of databases

Power: The information on thermal power plants was from Global Coal Plant Tracker [38] and World Electric Power Plants Database [215]; the information on hydropower was from GRanD v1.3 [216] and Liu et al. [204]. For the cooling system of thermal power plants, we used Google satellite imagery cross-checked with information from the China Electricity Council [217]. According to previous studies [118, 366], it is easy to identify a power plant in a satellite image by visual inspection using the images of the cooling facilities. For example, recirculating cooling systems are equipped with cooling towers and air cooling systems are equipped with air cooling

islands; once-through cooling systems do not have such cooling equipment. It is also worth noting that indirect air cooling systems also have cooling towers, but with a different appearance that can be identified by visual inspection.

Transmission: For each province, the sum of electricity generation and imports should theoretically equal to the sum of electricity consumption and exports [220]. Due to statistical discrepancies, there are small differences of around 2% for each province (except for Hebei, Heilongjiang and Shaanxi where the difference is 3%). We do not consider transmission loss in this study, mainly due to data unavailability.

Water consumption and withdrawal: Water consumption and withdrawal within basins were obtained from the World Resources Institute Aqueduct database for the baseline year 2010 [53, 224]. By summing up the water consumption/withdrawal of each basin, we get the national total water consumption/withdrawal assessed by the Aqueduct database in 2010, denoted by A. We also get the total amount of water consumption/withdrawal in 2017 from the National Bureau of Statistics [201], denoted by B. And then we can get the ratio between B and A, denoted by C. The water consumption and withdrawal of each basin in our study (2017) was obtained by multiplying the corresponding basin's water consumption/withdrawal in 2010 by C.

7.3 Supplementary information to chapter 4

S7.3.1 Estimates of water consumption

We assessed the provincial water consumption factors for thermal power and hydropower generation using the method in Jin et al. [16]. Based on the factors, the water consumption of electricity generation in each year is calculated as follows:

$$WC = \sum_i WC_i = \sum_i (TWC_i + HWC_i) = \sum_i (TF_i \cdot TP_i + HF_i \cdot HP_i) \quad \text{(S7.3.1)}$$

In which, WC gives the national water consumption for electricity generation (m^3); WC_i the water consumption for electricity generation in provinces i (m^3); TWC_i the water consumption for thermal power generation in province i (m^3); HWC_i the water consumption for hydropower generation in province i (m^3); TF_i the water consumption factor for thermal power generation in province i (m^3/GWh); HF_i the water consumption factor for hydropower generation in province i (m^3/GWh); TP_i the thermal power generation in province i (GWh); HP_i the hydropower generation in province i (GWh).

S7.3.2 Characterization factors for water consumption

Water consumed for electricity generation is not returned to the river. The influence of reduced flow rates on aquatic biodiversity can be quantified with the global species-discharge model, an index of habitat space, feeding and reproductive opportunities. This model is developed based on native fish species and river discharges in various river basins [274]. This model assumes a positive correlation between the number of freshwater fish species and average river discharges at the mouth of river basins.

$$R = 4.2 \cdot Q_{mouth,i}^{0.4} \quad \text{(S7.3.2)}$$

Where R is the freshwater fish species richness and $Q_{mouth,i}$ is the annual average river discharge at the river mouth of basin i (m^3/s).

The species-discharge relationship can be used to calculate characterization factors for water consumption that specify freshwater fish species loss per unit of reduced river discharge for river basins in different regions. Characterization factors (CF_c) for water consumption reflect the impact of water use due to human activities on freshwater biodiversity loss.

$$CF_{c,i} = FF_i \cdot EF_i = \frac{dQ_{mouth,i}}{dW_i} \cdot \left(\frac{dPDF_i}{dQ_{mouth,i}} \cdot V_i\right) \quad \text{(S7.3.3)}$$

Where FF_i is the fate factor of river basin i, EF_i is the effect factor of river basin i ($PDF \cdot m^3 \cdot yr \cdot m^{-3}$), $dQ_{mouth,i}$ is the marginal change in water discharge at the river mouth in basin i ($m^3 \cdot yr^{-1}$), dW_i is the marginal change in water consumption by human activities in river basin i ($m^3 \cdot yr^{-1}$), $dPDF_i$ is the marginal change in the potentially disappeared fraction of the freshwater fish species due to the marginal river discharge change $dQ_{mouth,i}$ and V_i is the volume of river basin i (m^3). The $dQ_{mouth,i}/dW_i$ is assumed to be equal to one, indicating that a change in water consumption is fully reflected in a change in water discharge at the mouth for that river basin.

$$\frac{dPDF_i}{dQ_{mouth,i}} = \frac{dR_i}{R_i \cdot dQ_{mouth,i}} = \frac{4.2 \cdot 0.4 \cdot Q_{mouth,i}^{0.4-1}}{4.2 \cdot Q_{mouth,i}^{0.4}} = \frac{0.4}{Q_{mouth,i}} \quad \text{(S7.3.4)}$$

The river volumes (m^3) for all river basins are calculated according to Hanafiah et al. [276] as follows:

$$V_i = 0.47 \cdot \left(\frac{Q_{mouth,i}}{2}\right)^{0.9} \cdot L_i \quad \text{(S7.3.5)}$$

Where V_i is the water volume in river basin i (m^3), $Q_{mouth,i}$ is the discharge at the river mouth in basin i ($m^3 \cdot yr^{-1}$), Li is the length of river i (m).

China can be divided into the following river basins: Huaihe, Haihe, Yellow, Yangtze,

Pearl, Southeast, Southwest, Continental, Songhua and Liaohe river basins. The characterization factors are calculated for these river basins. Specifically, Qiantang and Min rivers are the representatives of the Southeast river basin. The characterization factors of Qiantang and Min river basins are calculated for Zhejiang and Fujian provinces since they are the largest river basins of the two provinces, respectively [282, 367]. Talimu is the largest river in the Continental basin, and its characterization factor is calculated for this basin. In terms of Southwest, Brahmaputra is the largest river basin of Tibet, and its characterization factor is calculated for Tibet [368]. Nandu river is the largest river of Hainan province, and its characterization factor is calculated for Hainan. The discharges at the river mouth and the river length are obtained from the Ministry of Water Resources [281-284].

S7.3.3 Thermal pollution of power production

S7.3.3.1 Thermal pollution from thermal power

In power plants with once-through cooling systems, water from a freshwater body is used to absorb heat from the working fluid in the condenser. The entire volume of heated water is then discharged back into the water body. In the Rankine cycle of steam-electric generating units, pumps and boilers add heat to liquid water, which is converted into steam during that process. The high-pressure steam then expands in the turbine producing power. Upon exiting the turbine, the steam passes through the condenser where heat is rejected from the system turning the working fluid into a saturated liquid, ready to re-enter the pump. To calculate the rate of heat rejected in each cycle, the difference in enthalpy of the working fluid on either side of the condenser must be multiplied by the steam flow rate. The thermal pollution to water bodies from thermal power is calculated using the method of Raptis and Pfister [267]. The heat rejection rates of thermal power are assessed as follows:

$$Q_t = LF \cdot m_{steam}(h_b - h_a)/1000 \quad \text{(S7.3.6)}$$

Where Q is the heat rejection rate (MW), LF is the load or capacity factor of electricity generating units, which are derived from Jin et al. [8], m_{steam} is the steam flow rate at the high-pressure turbine (kg/s), h_b-h_a is the difference in enthalpy of the working fluid on either side of the condenser (kJ/kg).

The steam flow rate can be calculated as:

$$m_{steam} = \beta \cdot C_{gross} \quad \text{(S7.3.7)}$$

Where C_{gross} is the gross generating capacity (MW) and β is a constant (0.830 kg s^{-}

^{1} MW^{-1} [267]).

Reheat cycles can be added into the Rankine cycle, increasing the generation efficiency and thus reducing fuel inputs. When reheat cycles are employed, the steam passes first through a high-pressure turbine and, after being reheated, through a low-pressure turbine. 94% of China's units with an installed capacity of 100-220 MW use a reheat system, whereas all 300-1000 MW units use a reheat system [217]. For a reheat system, the ratio (r) of the steam flow at the entry of low-pressure turbine to the steam flow at the entry of high-pressure turbine is inserted to scale the rejection rate:

$$Q_t = LF \cdot m_{steam} \cdot r \cdot (h_b - h_a)/1000 \quad \text{(S7.3.8)}$$

Where r=0.85 is used for China's units in this study, referring to Yan et al. [369] and Cheng et al. [370]. h_a is related to the water temperature withdrawn for use in the condenser [267]. An additional necessary piece of information for all thermodynamic cycles is the temperature of the freshwater withdrawn for use in the condenser. To obtain these values, the georeferenced power plants are overlaid onto gridded estimates (at 10 km spatial resolution) of water temperatures [371]. The average over 15 years (2000-2014) is used to minimize the impacts of very warm or very cold years on the water temperature estimates. For every generating unit then, mean monthly naturalized water temperatures are extracted. The information on power plants is sourced from the China Electricity Council [217], Global Coal Plant Tracker [38], World Electric Power Plants Database [215] and our previous study [8]. The results of plant-level thermal pollution and its impacts are then aggregated to the provincial level.

S7.3.3.2 Thermal pollution from hydropower

Hydropower also produces heat during operation, though its thermal pollution is smaller than that of thermal power with a once-through cooling system because of its higher energy efficiency. The thermal emission of hydropower can be calculated as follows:

$$Q_h = LF \cdot C_{gross} \cdot HR \quad \text{(S7.3.9)}$$

Where HR is the heat emission rate of China's hydropower, referring to Xu et al. [372] and Yan and Hao [373]; here, HR is 1.8%. The definitions of LF and C_{gross} are the same as those in Equations 7-9.

There are approximately 47,000 hydropower stations in China [298]. It is infeasible to

assess the thermal emission and biodiversity impacts at the plant level because of data limitations. We made assessments at the provincial level by changing equation 10 to 11:

$$Q_h = LF_p \cdot C_p \cdot HR \quad \text{(S7.3.10)}$$

Where LF_p is the provincial load or capacity factor of hydropower, C_p is the provincial installed capacity of hydropower (MW). The values of LF_p and C_p are obtained from the National Bureau of Statistics [218].

S7.3.4 Biodiversity impacts assessments

Biodiversity loss caused by freshwater consumption: Electricity generation can cause aquatic biodiversity loss because of its water use [61, 374]. Surface water consumption impacts aquatic biodiversity. Water consumption is translated to impacts on aquatic biodiversity by characterization factors expressed as a potentially disappeared fraction of species (unit: PDF m^3yr /m^3) [276].

$$WBL_i = WC_i \cdot CF_{c,i} \quad \text{(S7.3.11)}$$

Where WBL_i gives the biodiversity loss caused by water consumption for electricity generation in province i (PDF m^3 yr); WC_i the water consumption for electricity generation in province i (m^3); $CF_{c,i}$ the biodiversity loss per unit of water consumption for electricity generation in province i (PDF m^3 yr/m^3);

Biodiversity loss caused by thermal emissions: The factor of local biodiversity impacts from thermal emissions is obtained from Raptis et al. [61] .

The biodiversity loss caused by electricity generation is calculated as follows:

$$TBL_i = TBLT_i + TBLH_i = \sum_n Q_{t,n,i} \cdot TBF_{n,i} + Q_{h,i} \cdot PTBF_i \quad \text{(S7.3.12)}$$

Where TBL_i gives the biodiversity loss caused by thermal emissions of electricity generation in province i (PDF m^3 yr); $TBLT_i$ the biodiversity loss caused by thermal emissions from thermal power in province i (PDF m^3 yr); $TBLH_i$ the biodiversity loss caused by thermal emissions from hydropower in province i (PDF m^3 yr); $Q_{t,n,i}$ the thermal emissions from the thermal power plant n in province i (MJ); $TBF_{n,i}$ the biodiversity loss per unit of thermal emissions at the location of plant n in province i (PDF m^3 yr/MJ); n the thermal power plants with once-through cooling systems in province i; $Q_{h,i}$ the thermal emissions from hydropower in province i (MJ); $PTBF_i$ the biodiversity loss per unit of thermal emissions in province i (PDF m^3 yr/MJ); the characterization factors are derived from Raptis et al. [61], where global gridded freshwater thermal pollution CFs are assessed. We extract the gridded CFs for

thermal power and China's CFs for hydropower at monthly resolution.

S7.3.5 Estimates of water stress

The Water Stress Index is calculated according to Pfister et al. [375], which is adapted from the water withdrawal-to-availability indicator by applying a logistic function to acquire continuous values between 0.01 and 1. The equation is as follows:

$$WSI = \frac{1}{1+e^{-6.4 \cdot WTA^*}(\frac{1}{0.01}-1)} \quad \text{(S7.3.13)}$$

Where *WSI* is the water stress index. *WTA** is a modified *WTA* indicator considering the difference for watersheds with and without strongly regulated flows. Four levels of water stress are classified in the *WSI*, i.e. minor (0.01-0.09); moderate (0.09-0.5); severe (0.5-0.91); and extreme (0.91-1). The water stress indexes are calculated for 2017 based on the water withdrawal and availability from the Ministry of Water Resources [225].

S7.3.6 Converting local impacts to global impacts

Kuipers et al. estimated global extinction probabilities (GEPs) based on species range sizes, species vulnerabilities, and species richness, indicating to what extent regional species loss in the respective area may contribute to global species loss. They generate them for marine, terrestrial, and freshwater species groups on the local (i.e., 0.05° × 0.05° grid) and ecoregion scale [290]. The regional fractions of freshwater species losses are then multiplied with the corresponding GEPs to calculate potential global fractions of extinctions:

$$GBL_i = BL_i/V_i \cdot GEP_i \quad \text{(S7.3.14)}$$

Where GBL_i gives the potential global biodiversity loss in province *i* (PDF yr); V_i is the volume of the representative river in province *i*; GEP_i is the global extinction probability in province *i*, calculated by aggregating the cell-level GEPs from Kuipers et al. [290] within province *i*.

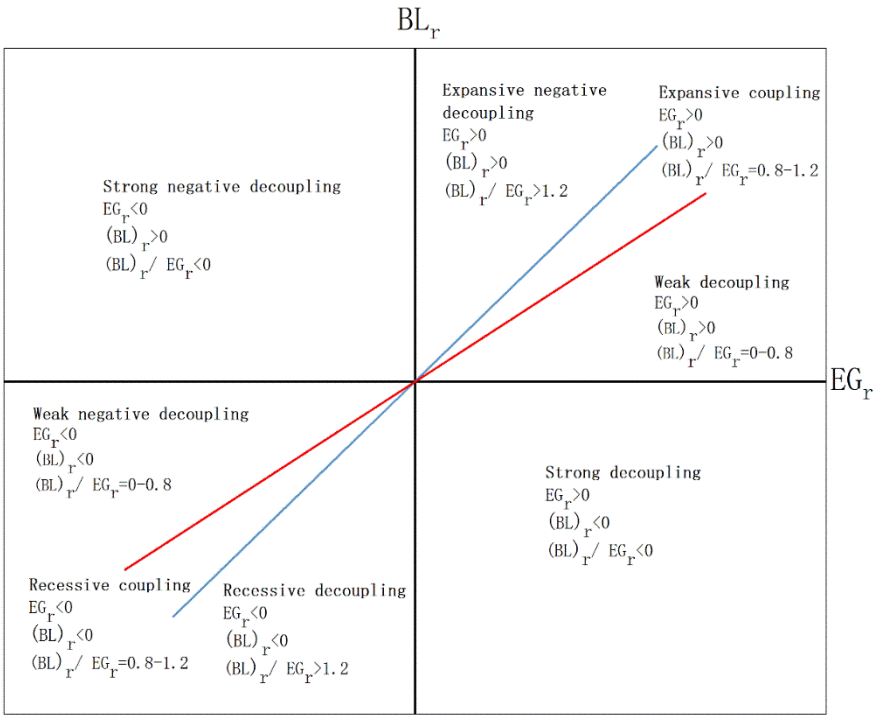

Figure S7.3.1 The decoupling state quadrant map corresponding to the decoupling degree. Here, $BL_r=\Delta BL/BL_{t-1}$, $EG_r=\Delta EG/EG_{t-1}$. This map is modified from Tapio [277].

Figure S7.3.2 China's provinces.

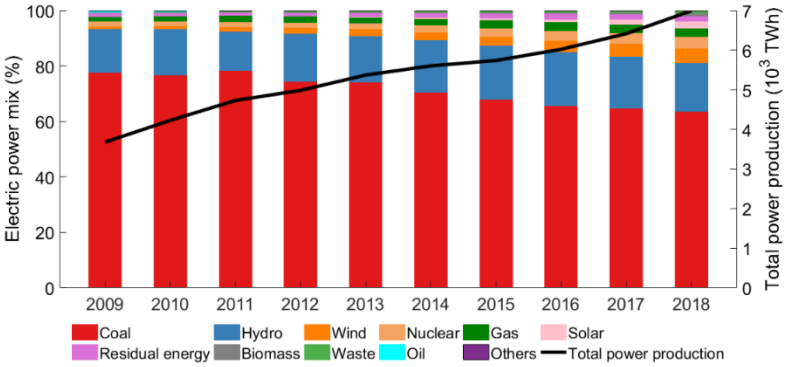

Figure S7.3.3 The electric power mix in China.

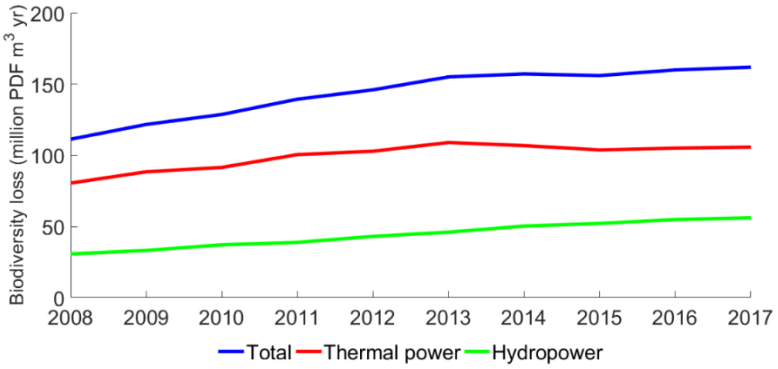

Figure S7.3.4 The biodiversity loss by freshwater use for China's electricity generation during 2008-2017.

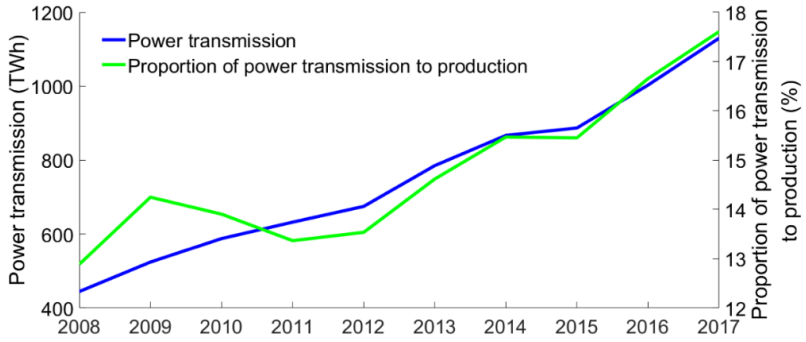

Figure S7.3.5 The total amount of interprovincial power transmission in China.

Table S7.3.1 The provincial characterization factors of water consumption impacts on local biodiversity.

Province	Characterization factor (PDF·m^3·yr·m^{-3})	Province	Characterization factor (PDF·m^3·yr·m^{-3})
Beijing	1.76E-03	Hubei	7.19E-03
Tianjin	1.76E-03	Hunan	7.19E-03
Hebei	1.76E-03	Guangdong	2.78E-03
Shanxi	8.17E-03	Guangxi	2.78E-03
InnerMongolia	8.17E-03	Hainan	5.79E-04
Liaoning	2.51E-03	Chongqing	7.19E-03
Jilin	2.84E-03	Sichuan	7.19E-03
Heilongjiang	2.84E-03	Guizhou	7.19E-03
Shanghai	7.19E-03	Yunnan	3.99E-03
Jiangsu	7.19E-03	Xizang	2.79E-03
Zhejiang	6.76E-04	Shaanxi	8.17E-03
Anhui	7.19E-03	Gansu	8.17E-03
Fujian	8.14E-04	Qinghai	8.17E-03
Jiangxi	7.19E-03	Ningxia	8.17E-03
Shandong	1.50E-03	Xinjiang	3.34E-03
Henan	1.50E-03		

Table S7.3.2 The provinces' full names and abbreviations used in Figure 4.4.

Full name	Abbreviation	Full name	Abbreviation
Anhui	AH	Liaoning	LN
Beijing	BJ	Inner Mongolia	NM
Fujian	FJ	Ningxia	NX
Gansu	GS	Qinghai	QH
Guangdong	GD	Shandong	SD
Guangxi	GX	Shanxi	SX
Guizhou	GZ	Shaanxi	SN
Hainan	HI	Shanghai	SH
Hebei	HE	Sichuan	SC
Henan	HA	Tianjin	TJ
Heilongjiang	HL	Xizang	XZ
Hubei	HB	Xinjiang	XJ
Hunan	HN	Yunnan	YN
Jilin	JL	Zhejiang	ZJ
Jiangsu	JS	Chongqing	CQ
Jiangxi	JX		

Table S7.3.3 The decoupling degree and decoupling state (see Figure S.7.3.1) between biodiversity loss and electricity generation.

Time period	Decoupling degree	Decoupling state
2008-2009	1.4	Expansive negative decoupling
2009-2010	0.39	Weak decoupling
2010-2011	0.7	Weak decoupling
2011-2012	0.87	Expansive coupling
2012-2013	0.8	Expansive coupling
2013-2014	0.31	Weak decoupling
2014-2015	-0.31	Strong decoupling
2015-2016	0.52	Weak decoupling
2016-2017	0.19	Weak decoupling

7.4 Supplementary information to chapter 5

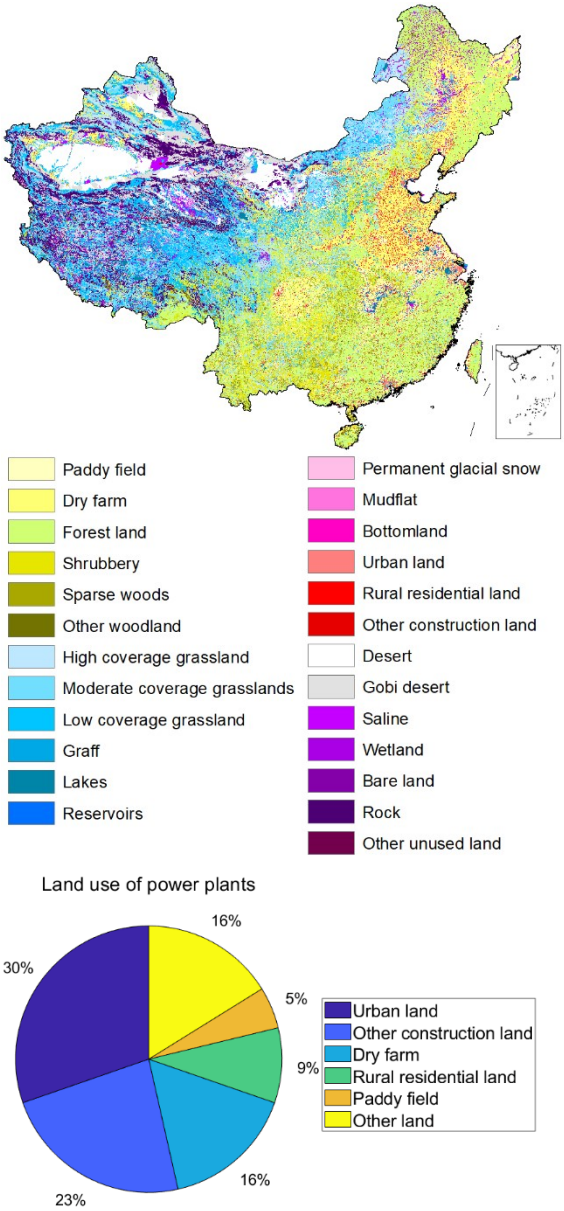

Figure S7.4.1 China's land use type (1km resolution) and the type of power plants' location. Data source: Resource and Environment Science and Data Center [376].

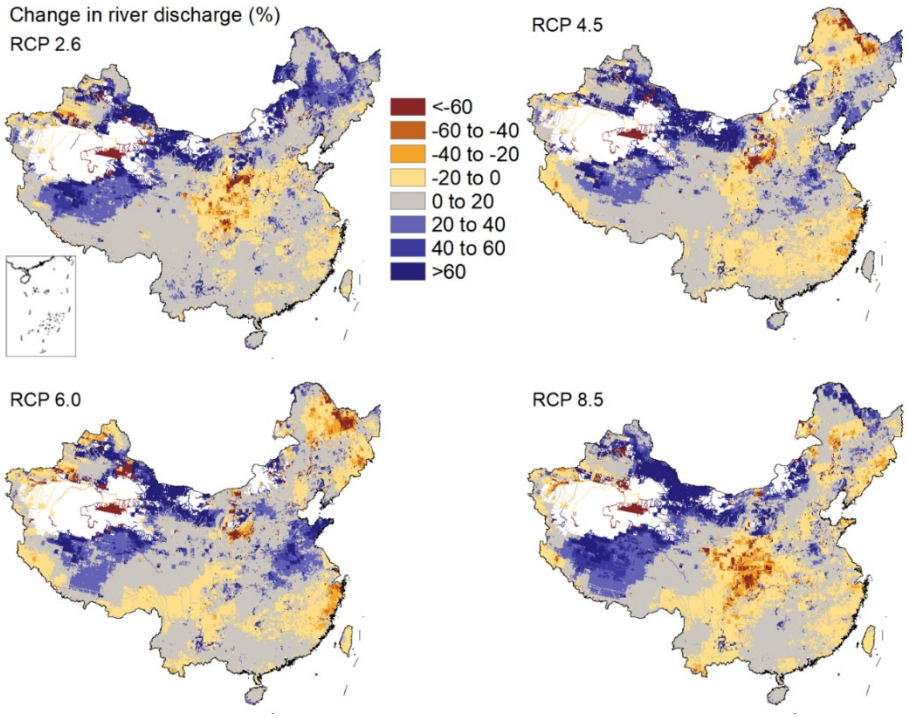

Figure S7.4.2 Impacts of climate change on annual average river discharge. Maps of changes in river discharge for climate scenarios RCP2.6, RCP4.5, RCP6.0, and RCP8.5 in the 2030s relative to the reference period.

Figure S7.4.3 Map (left) presents provinces and map (right) shows the major river basins.

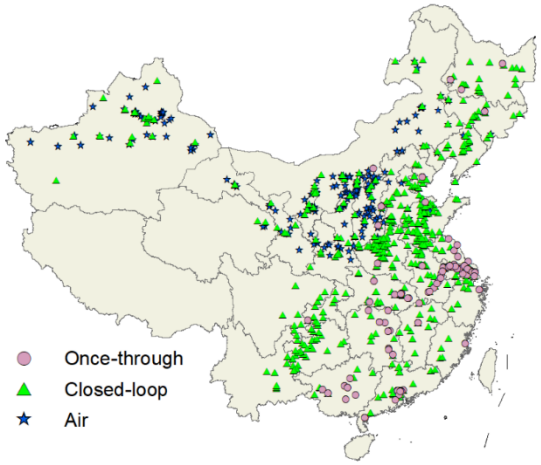

Figure S7.4.4 Coal-fired power plants' location and cooling type.

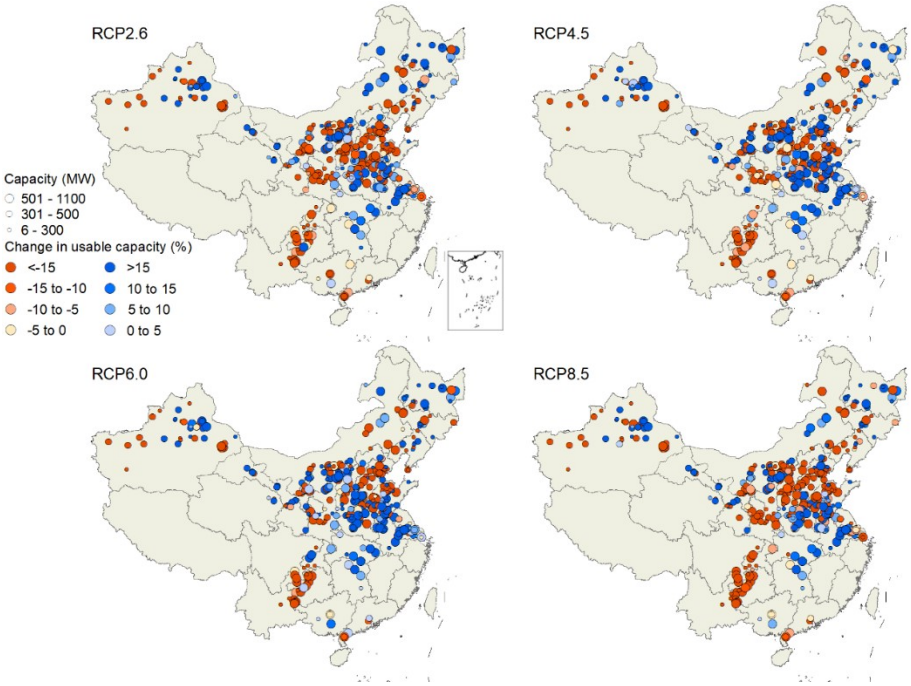

Figure S7.4.5 Impacts of climate and water resources change on usable capacity of CPUs in spring (March, April, May). The changes in the annual usable capacity under four climate scenarios in the 2030s compared to the reference period. Those that do not experience changes in usable capacity reductions are not shown on the maps.

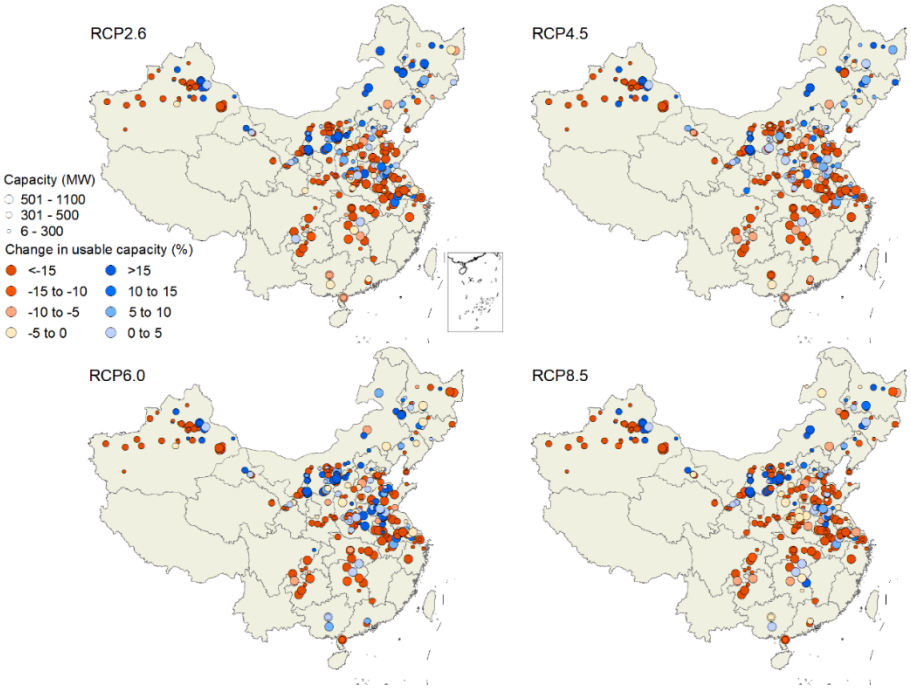

Figure S7.4.6 Impacts of climate and water resources change on usable capacity of CPUs in summer (June, July, August). The changes in the annual usable capacity under four climate scenarios in the 2030s compared to the reference period. Those that do not experience changes in usable capacity reductions are not shown on the maps.

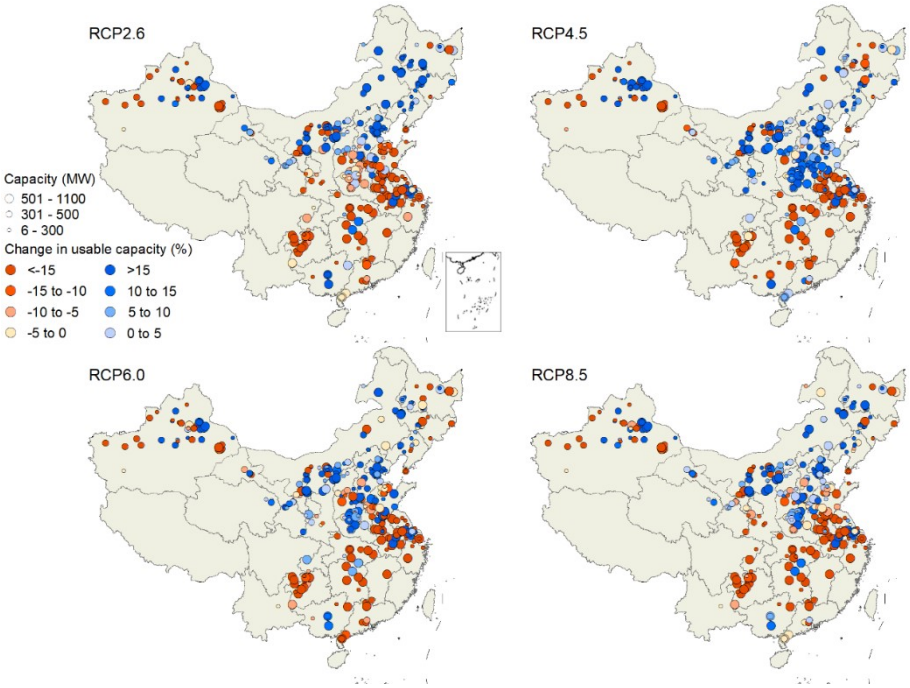

Figure S7.4.7 Impacts of climate and water resources change on usable capacity of CPUs in autumn (September, October, November). The changes in the annual usable capacity under four climate scenarios in the 2030s compared to the reference period. Those that do not experience changes in usable capacity reductions are not shown on the maps.

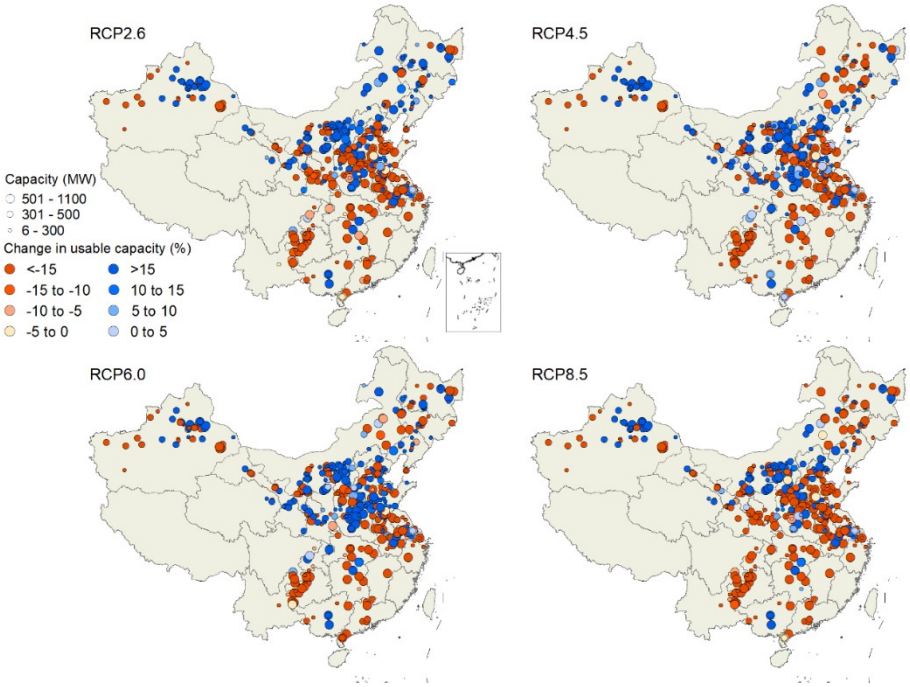

Figure S7.4.8 Impacts of climate and water resources change on usable capacity of CPUs in winter (December, January, February). The changes in the annual usable capacity under four climate scenarios in the 2030s compared to the reference period. Those that do not experience changes in usable capacity reductions are not shown on the maps.

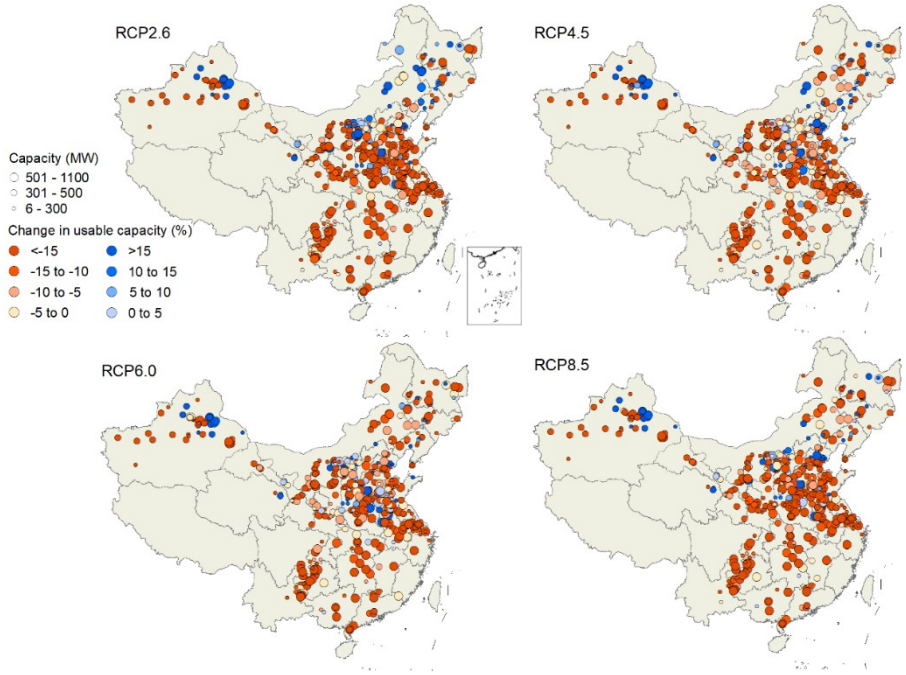

Figure S7.4.9 Impacts of climate and water resources change on annual usable capacity of CPUs with CCS. The changes in the annual usable capacity under four climate scenarios in the 2030s compared to the reference period. Those that do not experience changes in usable capacity reductions are not shown on the maps.

Table S7.4.1 The changes in provincial usable capacity under scenarios RCP2.6, RCP4.5, RCP6.0, and RCP8.5 for the 2030s relative to the reference period. Unit: MW

	RCP2.6	RCP4.5	RCP6.0	RCP8.5
Anhui	-85	-4	428	-141
Beijing	108	110	111	109
Chongqing	-147	-15	18	-359
Fujian	0	0	0	0
Gansu	42	266	520	-7
Guangdong	-512	-665	-567	-451
Guangxi	75	-136	-15	-57
Guizhou	-1921	-2974	-2846	-3573
Hebei	1048	1589	1250	614
Heilongjiang	1081	653	392	563
Henan	-540	1100	1586	-166
Hubei	-279	-95	-31	-529
Hunan	-54	-208	-121	15
Inner Mongolia	3797	2168	1530	2190
Jiangsu	346	754	908	334
Jiangxi	-457	-427	-472	-464
Jilin	312	157	-56	-81
Liaoning	213	397	107	-33
Ningxia	101	275	266	260
Qinghai	184	199	198	195
Shaanxi	-2047	-1273	-873	-2302
Shandong	-2820	15	1161	-2488
Shanghai	-16	-7	4	-23
Shanxi	-1021	242	689	-1055
Sichuan	-432	-315	-192	-978
Tianjin	85	690	-96	82
Xinjiang	4816	5417	3610	5030
Yunnan	-322	-967	-705	-1148
Zhejiang	-289	-477	-486	-492

Table S7.4.2 The changes in provincial usable capacity when CCS is implemented under scenarios RCP2.6, RCP4.5, RCP6.0, and RCP8.5 for the 2030s relative to the reference period. Unit: MW

	RCP2.6	RCP4.5	RCP6.0	RCP8.5
Anhui	-1495	-1269	-997	-1505
Beijing	57	58	56	52
Chongqing	-795	-696	-684	-963
Fujian	0	0	0	0
Gansu	-1010	-923	-699	-1098
Guangdong	-1338	-1578	-1444	-1362
Guangxi	-335	-494	-379	-372
Guizhou	-4405	-5327	-5136	-5708
Hebei	-588	-97	-440	-1019
Heilongjiang	-414	-860	-1047	-880
Henan	-4495	-2830	-2515	-4095
Hubei	-721	-576	-453	-932
Hunan	-852	-973	-886	-801
Inner Mongolia	-165	-2327	-2575	-1745
Jiangsu	-2857	-2524	-2250	-2815
Jiangxi	-494	-601	-539	-524
Jilin	-206	-335	-484	-491
Liaoning	-364	-206	-484	-583
Ningxia	-600	-404	-411	-485
Qinghai	107	115	115	109
Shaanxi	-3279	-2304	-2033	-3381
Shandong	-5343	-2744	-1817	-5161
Shanghai	-73	-64	-63	-79
Shanxi	-3445	-2270	-1721	-3646
Sichuan	-1181	-981	-784	-1727
Tianjin	-232	266	-354	-289
Xinjiang	2351	2513	829	2441
Yunnan	-1108	-1792	-1620	-1950
Zhejiang	-620	-758	-738	-732